

Stochastic Geometry-based Analysis for Cooperative Multi-hop Networks



By

Muhammad Ahsen

2013-NUST-MS-EE-05

Supervisor

Dr. Syed Ali Hassan

Department of Electrical Engineering

A thesis submitted in partial fulfillment of the requirements for the degree
of Masters of Science in Electrical Engineering (MS EE)

In

School of Electrical Engineering and Computer Science,
National University of Sciences and Technology (NUST),

Islamabad, Pakistan.

(February 2016)

Approval

It is certified that the contents and form of the thesis entitled “**Stochastic Geometry-based Analysis for Cooperative Multi-hop Networks**” submitted by **Muhammad Ahsen** have been found satisfactory for the requirement of the degree.

Advisor: Dr. Syed Ali Hassan

Signature: _____

Date: _____

Committee Member 1: Dr. Rizwan Ahmad

Signature: _____

Date: _____

Committee Member 2: Dr. Sajid Saleem

Signature: _____

Date: _____

Committee Member 3: Dr. Hassaan Khaliq

Signature: _____

Date: _____

Abstract

A strip-shaped multi-hop network with random node locations is analyzed using a spatial Poisson point process (PPP) and stochastic geometry tool for single-input single-output (SISO) links and for virtual multiple-input single-output (MISO) links, which are usually formed in cooperative transmission. A decode-and-forward (DF) protocol is considered for MISO transmissions over the multi-hop network forming Opportunistic Large Array (OLA). A closed-form expression for the probability density function (PDF) of the received power at a node is derived for both SISO and MISO links which further characterizes the performance of the network. The power received at a node in SISO links, when a randomly deployed transmitter transmits the message signal in the presence of Rayleigh fading and random path loss, is shown to be the ratio of an exponential random variable (RV) and a generalized gamma (GG) RV. The cumulative distribution function (CDF) of the ratio is derived, which is used to find the coverage probability at the receiver. For the PDF of the received power in MISO links, the distribution of the Euclidean distance between a pair of nodes in adjacent hops is derived, which by invoking the method of moments, is approximated by the Weibull distribution. The Weibull distribution is then used to calculate the PDF of the received power, provided that all DF nodes transmit with same power under a Rayleigh fading channel. The notions of one-hop success probability and coverage range

are analyzed for various network parameters. An algorithm for conserving energy in multi-hop OLA network for MISO links by using thinning in PPP is also proposed and its performance in terms of the fraction of energy saved (FES) is quantified. It is shown that the proposed algorithm is more energy efficient as compared to an independent thinning algorithm.

To my parents.

Certificate of Originality

I hereby declare that this submission is my own work and to the best of my knowledge it contains no materials previously published or written by another person, nor material which to a substantial extent has been accepted for the award of any degree or diploma at NUST SEECS or at any other educational institute, except where due acknowledgement has been made in the thesis. Any contribution made to the research by others, with whom I have worked at NUST SEECS or elsewhere, is explicitly acknowledged in the thesis.

I also declare that the intellectual content of this thesis is the product of my own work, except for the assistance from others in the project's design and conception or in style, presentation and linguistics which has been acknowledged.

Author Name: **Muhammad Ahsen**

Signature: _____

Acknowledgment

I am grateful to my family who have always motivated me and supported me. They have taught me how to deal with difficult problems and enable me to achieve this milestone in my life.

I would like to thank Dr. Syed Ali Hassan for his continuous support, guidance and encouragement. He is a source of inspiration for me, who have never let me down during my dissertation work.

Finally, I would like to thank my committee members: Dr. Sajid Saleem, Dr. Rizwan Ahmad and Dr. Hassaan Khaliq and my friends who have helped me through this phase of life.

Table of Contents

1	Introduction	1
1.1	Cooperative Diversity	1
1.2	Opportunistic Large Array	3
2	Background and Literature Review	6
2.1	Modeling Cooperative Transmissions	6
2.2	Distance Distribution	9
2.3	Energy Efficiency in OLA	10
3	Network Architecture	13
3.1	System Model	13
3.2	Membership of a Node	16
3.3	Received Power	16
4	SISO Links	17
4.1	Ratio of an exponential RV and GG RV	19
4.2	Coverage Probability	22
5	Virtual MISO Links	23
5.1	Virtual MISO links with Hypothetical Boundaries	23

<i>TABLE OF CONTENTS</i>	viii
5.2 Distance Distribution between a pair of nodes without any Hypothetical Boundary	26
5.3 Virtual MISO Links with Irregular Hop Boundaries	32
6 Energy Efficiency	33
7 Results and Discussions	38
7.1 SISO Links	38
7.2 MISO Links	43
8 Conclusion and Future Direction	55

List of Figures

1.1	Space Diversity	2
1.2	Cooperative Diversity	2
3.1	A 2D strip-shaped network with finite node density.	14
3.2	Formation of levels along with membership probability.	14
3.3	Transmission of signal from one hop to another without a fixed hypothetical boundary. A single node constitutes a MISO scenario.	15
4.1	Transmission of signal from one node to another without fixed boundary	17
5.1	A strip-shaped network with hypothetical boundaries and ran- dom node locations.	24
5.2	A realization of a pair of nodes placed randomly in adjacent levels.	28
6.1	Two subsets of transmitters.	34
6.2	Thinning of PPP.	36
7.1	CDF of the ratio for $k = 2$, $\theta = 15^\beta$, $\omega = 1$ and $\beta = 0.8, 1, 2$. . .	39
7.2	CDF of the ratio for $k = 1$, $\theta = 1$, $\omega = 1$ and $\beta = 0.8, 1, 2$. . .	40

7.3	Coverage probability of a SISO link for $k = 1$, $\omega = 1$, $\alpha = 2$ and $\beta = 1$	41
7.4	Hop count for $k = 1$, $\omega = 1$, $\alpha = 2$, $\beta = 1$ and $\eta = 0.8$	42
7.5	Effect of nearest communicating node on the coverage probability for $\lambda = 1$, $\omega = 1$, $\alpha = 2$ and $\beta = 1$	43
7.6	Outage probability for virtual MISO with hypothetical boundaries for $P_t = 1$, $L = 2$ and $\alpha = 2$	44
7.7	Membership probability in three adjacent levels virtual MISO with irregular hop boundaries for $B = 8$, $\tau = 0.04$, $\alpha = 2$	46
7.8	Comparison of the simulation distance distribution with the Weibull distribution for virtual MISO with irregular hop boundaries $B = 4$, $\Delta = 2$ and $\alpha = 2$	47
7.9	Comparison of the coverage probability of a node for MISO without hypothetical boundaries using analytical and simulation model for $B = 4.69$, $\mu = 1.17$, $\Delta = 1.45$, $P_t = 1$ and $\alpha = 2$	48
7.10	Effect of the average number of nodes on one-hop success probability with $\alpha = 2$, $\mu = 2.62$, $\Delta = 2.12$ and $B = 7.87$	49
7.11	Coverage range for different values of transmit power, P_t , and average number of nodes, γ with $\mu = 4.05$, $\Delta = 1.27$, $B = 9.75$, $\eta = 0.8$ and $\tau = 0.2$	50
7.12	FES for three different values of γ with $\mu = 5$, $\psi = 14dB$, $B = 6$, $\eta = 0.8$, and $\Delta = 2$	51
7.13	Comparison of the Th-OLA with the independent thinning process for $\psi = 14dB$, $\gamma = 8$, $\mu = 5$, $\Delta = 2$, $\eta = 0.8$ and $B = 6$	54

List of Tables

2.1	Cooperative Diversity Protocols	7
7.1	Effect of hop distance on FES	53

Chapter 1

Introduction

1.1 Cooperative Diversity

Diversity in the transmission of information over wireless channels is a way to combat fading. Diversity can be applied through multiple antennas separated in space so that the receiver can have the multiple copies of the same signal, transmitted over the independent fading paths. It can also be provided through multiple time slots (temporal diversity) or multiple frequency channels where the same information is sent through the multiple time slots or the multiple frequency channels. Combining technique is applied at the receiver side to take advantage from the multiple copies of the signal. Another diversity technique known as cooperative diversity, was introduced in [1]. It is based on the relaying of the source information towards the destination [2]. With this technique distant receivers can be communicated effectively and efficiently.

Cooperative diversity is a specific case of the spatial diversity in which the transmitter of another user is used for relaying the signal. Spatial diversity requires two transmitters to be installed at specific distance from each other

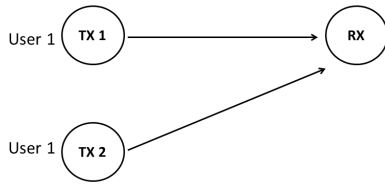


Figure 1.1: Space Diversity

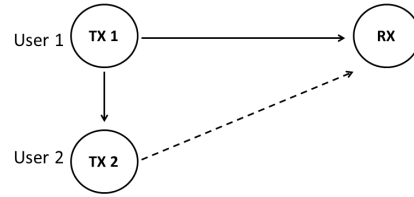


Figure 1.2: Cooperative Diversity

so that independent fading paths can be exploited as seen in Figure 1.1. For spatial diversity, each user has a minimum of two transmitters. In cooperative diversity, second transmitter does not belong to the user one but it belongs to the second user and it cooperates in transmitting the signal of the user one as shown in Figure 1.2. In either of the cases, receiver is getting minimum of the two copies of each signal. The benefit of the independent fading path is that one of the two copies of the signal may undergo severe fading but other copy might not, as it is highly unlikely that both independent fading paths are facing severe fading conditions simultaneously. It can also help in reaching the distant destination without draining the power of the user one, which will otherwise be drained. In spatial diversity an antenna array is to be established, whereas in cooperative diversity a virtual array is established.

It is a very useful technique for wireless communication whether single hop communication or multi-hop with strong dependence on the node density for the success [3]. It can be employed for different purposes either increasing the range or the data rates. Increasing the data rates is one of the requirements of the higher generation cellular networks and higher generation networks are the need of today. Applications like voice over IP (VOIP) and any other data hungry applications can take advantage from the cooperative communication.

Cooperative communication improved the reliability of the wireless communication. It was implemented in different ways in the cellular systems such

as DAS (Distributed Antenna System) in which two antennas located at the different locations transmit the same information [?]. Other techniques were Multi cell coordination and Coordinated Multiple Point (CoMP). All of these techniques offer significant advantages over wireless channels as compare to old techniques.

1.2 Opportunistic Large Array

Opportunistic Large Array (OLA) is a form of cooperative transmission (CT) [5], where multiple nodes transmit the same message after successful decoding, without any coordination among each other and without any addressing scheme. A promising characteristic of this technique is that it does not require any prior information of the number of cooperating nodes or their locations, which makes it a scalable technique and suitable for transmission without any cluster head. This technique is well efficient in unicasting the message to a desired destination or broadcasting the data to the entire network. In basic OLA every other node that receives the signal, retransmits that signal in the next time slot if it satisfies the following two conditions

- Received signal has optimum signal-to-noise (SNR) for decoding
- Node has not transmit the same signal before.

It can be used in number of the application like smart grid where each node sends it data to the central station and the central station sends back some information. This type of the network has two requirements other than the reliable communication, i.e., reaching distant central station and extending network life by extending the life of the batteries. OLA is successful in meeting these demands along with the basic requirement of the reliable

communication. Sensor network is the popular choice for monitoring health, pollution, waste disposal and many others. All such applications require longer battery life and reliable communication. OLA can be used in all such applications and in many cases, variants of the OLA are used for conserving energy.

In this work, we study the random behavior of the nodes in a strip-shaped OLA network with finite node density and presents a stochastic transmission model besides proposing an energy conservation algorithm. The considered network is a general network, where the number of nodes per hop are random along with random node placements and irregular hop boundaries. The transmission model resembles a typical OLA, where the transmission of the signal from a source to a distant destination forms irregular levels or hops characterizing random number of nodes in each hop.

Our stochastic model is based on the theory of Poisson point process (PPP) [6], where random number of nodes in each hop are independent and distributed according to a Poisson random variable (RV). The analytical tractability of the PPP makes it a suitable candidate to model the random number of nodes in each hop; unlike fixed number of nodes, which can be generally modeled using quasi-stationary Markov chains [7]. Once modeled, void probability of PPP is used to compute various network performance metrics such as m -hop success probability, coverage range (CR) and required node density to achieve a particular CR under a quality of service (QoS) constraint.

The geometric complexity of the system increases with the randomness of the nodes and irregular hop boundaries and the path loss becomes a random function. The path loss is dependent upon the actual Euclidean distance between the nodes, which when combined with fading provides the notion

of signal-to-noise ratio (SNR) for a single link. In CT, multiple single-input single-output (SISO) links are averaged over a PPP to analyze multiple-input single-output (MISO) links. Our main contributions in this paper are the followings.

- Derivation of the distribution of the received power for the SISO links.
- Derivation of the distribution of the received power for the virtual MISO links with hypothetical boundaries in between the hops, which is the random sum over a PPP of the ratio of an exponential random variable (RV) and a Weibull RV.
- Derivation of the distribution of the Euclidean distance between a pair of nodes distributed randomly in adjacent overlapping levels without any hypothetical boundary in between them.
- It is shown with the help of some statistical approaches such as the moment matching method that the distribution of the distance raised to a positive power can be well approximated by a Weibull distribution.
- We derive the distribution of the received power for a virtual MISO link with irregular hop boundaries.
- We devise a thinning of PPP to conserve energy for the finite node density OLA networks with random node placements by allowing only a subset of nodes to transmit and quantify its performance.

Chapter 2

Background and Literature Review

2.1 Modeling Cooperative Transmissions

This chapter is all about the literature associated with the cooperative diversity and the opportunistic large array (OLA) and comparisons from the other algorithms used for the similar functions. Initially cooperative diversity was exploited to achieve diversity gain using single relay based on any of the schemes presented in [2], as shown in table 2.1.

Each protocol has its own merits and demerits along with different requirements. In amplify and forward protocol, relaying node amplifies the signal and forwards it without performing error check. It was successful in achieving the diversity gain of the second order. In decode and forward protocol, relaying node will forwards the signal after decoding it. However, it will not check the correctness of the decoded signal and may forward the corrupted signal, which results in the loss of the diversity gain. Selection decode and forward protocol solves this problem as it forwards only those

Table 2.1: Cooperative Diversity Protocols

Relaying scheme	Protocol	Diversity gain
Fixed Relaying Scheme	Amplify and forward	Second Order
Fixed Relaying Scheme	Decode and forward	First Order
Selection Relaying Scheme	Selection Decode and forward	Second Order
Incremental Relaying Scheme	Incremental Amplify and forward	Second order

signals which it has decoded correctly and attain diversity gain. Incremental amplify and forward needs feedback from receiver that whether relaying is required or not.

Cooperative networks were studied with different perspectives such as channel capacity [8], outage behavior [9], receiver designs to reduce bit error rate (BER) [10] and use of multiple relays to extend the range in [11] and [12]. Authors in [13] and [14], studied the selection of the best possible relay (nearer to the destination).

Later concept of many relays was introduced for single source. In which every other node echoes source transmitted sequence forming large array known as opportunistic large array (OLA) [5]. In OLA, intermediate nodes relay source's signal in the form of a Mexican Wave. Techniques that were used before the OLA require regeneration, which is not an easy task to accomplish. It involves complex and costly system. Other techniques involve

pre-route allocation and addressing schemes, which require larger overheads (involvement of higher layers) [15] and need lots of the processing power. The use of the addressing scheme requires buffers for storing the sequences. These parameters restrict the networks scalability. Whereas in OLA, there is no need of such things making it much more scalable, simple and easy to implement. It is because of these features that make OLA a suitable choice for flooding in wireless sensor networks (WSNs) as it only use lowest layer (physical layer) for routing. OLA is different from CT, as in CT relaying nodes are pre-selected whereas in OLA they are selected on the basis of the two conditions previously discussed [9].

Other routing algorithm which involves pre-route allocation and addressing is known as Proteus [3]. It is a two-step process, first is the route allocation after feedback from destination and second is the actual transmission of data. If somehow allocated route broke then new route has to be allocated for the transmission. It is a connection oriented approach which ensures reliability and throughput but involves the complexity of the route allocation and the addressing.

Delay is an important parameter when receiver has multiple copies of the signal. To keep the delay between multiple copies at its minimum is the primary requirement, so each layer nodes transmit the signal at distinct time slots [16]. Authors in [17], have studied this behavior and quantified the number of the relays per hop and minimum SNR margin required for limiting the synchronization errors.

The authors in [18] modeled a strip-shaped network with infinite node density and presented their results in terms of the successful signal reception at a distant receiver. Their results, however, cannot be applied to the network with lesser node density [19]. It is also shown in [20] that the infinite propa-

gation is forbidden in the case of the finite node density. The authors in [21] and [22] showed that for the finite node density, infinite propagation is not possible, however data can be propagated to a destination node using the notion of success probability. OLA has become a very rich field and researchers have analyzed this field through various perspectives [23–26]. In [27], authors study the linear finite node density network with random node placement. Random placements of nodes were modeled by a Bernoulli random variable (RV) and proved that random placement of nodes degrades the SNR. The strip-shaped network with fixed number of nodes in each level with random node placement was studied in [28]. The model presented in [28] successfully cater the problem of random locations of nodes in each level but their main restriction was the fixed number of nodes in each level and fixed hop boundaries. Quasi-stationary markov chain was used to model the fixed number of the nodes per level in [29] and [30]. However, random node locations and finite node density are not addressed jointly.

2.2 Distance Distribution

The randomness of the nodes and irregular hop boundaries make path loss a random function. The path loss is dependent upon the actual Euclidean distance between the nodes. In [31], authors present a detailed survey on the distribution of distance for a PPP and for nodes which are independently and uniformly distributed. For multiple dimensional network, generalized gamma (GG) distribution is used to model the distance in PPP [32]. This distribution is useful in modeling the transmissions in SISO links, however, this distribution is not valid for a MISO link, where group of nodes form one level. The authors in [33] derived the distance distribution for nodes

present in adjacent square regions. However, the distribution of the Euclidean distance for nodes present in adjacent levels with irregular hop boundaries does not exist in the technical literature to the extent of our knowledge.

2.3 Energy Efficiency in OLA

Broadcasting in multi-hop networks is required to be energy efficient as the energy resources of the sensor networks are limited. Basic OLA wasn't enough for conserving the energy as every other node relay source information, which may be not required in multi-hop network [34]. OLA with threshold (OLA-T) was proposed to conserve the transmit energy by allowing only limited number of the nodes to cooperate [35]. It is a signal-to-noise ratio (SNR) based threshold. Only those nodes will take part in CT whose received SNR is lower than threshold τ_u and greater than lowest SNR threshold τ_l , which is required for the error free decoding of the received signal. So basically, the range of the SNR is defined and if the received SNR falls in that range the node will relay the signal otherwise it will not [36] and [37]. Range of the SNR has a direct impact on the cooperation of the nodes and on the success rate of the OLA. Energy efficiency is totally dependent on the node deployments.

OLA-T has some limitations [38] that its relaying nodes remain same for a longer period of time which will drain the batteries of the relaying nodes and batteries of the non-relaying nodes are not used in this case. OLA-T was conserving the energy when compared with the OLA but it was not utilizing the resources efficiently. This deficiency was termed as network hole by the authors. A new algorithm called Alternating OLA with transmission threshold (A-OLA-T) [39] was presented to overcome this deficiency. Main

aim of this algorithm is that somehow relaying nodes and non-relaying nodes swap their operation for next round of transmission i.e. transmission window for relaying keeps on changing on the regular intervals. This is more or what load balancing algorithm, i.e., distribute the operation of relaying among all nodes in the subsequent transmissions. It also extends the battery life and in turn network life by efficiently utilizing the different nodes for relaying in subsequent transmissions.

Both these algorithms OLA-T and A-OLA-T are used for broadcasting in the downstream domain. For upstream, another algorithm was presented which relies on concentric rings formed by OLA. This algorithm is known as Opportunistic Large Array Concentric Routing Algorithm (OLACRA) [40]. Concentric Rings are formed in the downstream direction from the node, which will be a sink (destination) in the upstream by the OLA. After every ring there is a change in the waveform to keep track of the rings. Then upstream cooperation takes place by utilizing these rings. A variant of this is OLACRA with threshold (OLACRA-T).

The results of the energy conserving algorithms were quite convincing but they were not valid for sparse node density networks as they basically relied on the assumption of *continuum* of nodes. For finite node density network, OLA with limited participation (OLA-LP) was proposed to conserve energy [41] with deterministic node placement. Markov chain was used to study the fixed number of the nodes and energy conservation by limiting the relaying nodes in each layer. And they proposed threshold based or SNR based algorithm for limiting the number of relaying nodes. However, practical environment involves finite node density and random placement of the node. In this work, we propose an energy conserving algorithm for finite node density with random node placements, hence a step closer to practical

situations.

Chapter 3

Network Architecture

In this chapter, we present the network architecture and assumptions used for modeling the cooperative multi-hop network.

3.1 System Model

Consider a strip-shaped 2-dimensional (2D) network with a finite node density where the node locations are random as shown in Fig. 3.1. A hop or level is formed opportunistically by a group of decode-and-forward (DF) nodes that successfully decode the signal, transmitted by a source node or a group of the nodes in the previous level. The DF nodes retransmit the same signal to the nodes ahead in the next time slot. Initially, for the first time slot, the source node transmits the signal, which is received by a group of nodes in the proximity and a subset of nodes decodes the message successfully depending upon transmit power, decoding threshold and nodes density. The nodes that successfully decode the signal become members of the level or hop 1. The DF nodes at level 1 transmit the same signal in the next time slot cooperatively and level 2 is formed. This process continues and

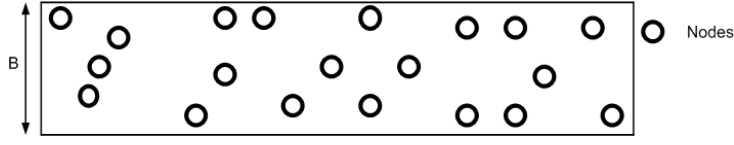


Figure 3.1: A 2D strip-shaped network with finite node density.

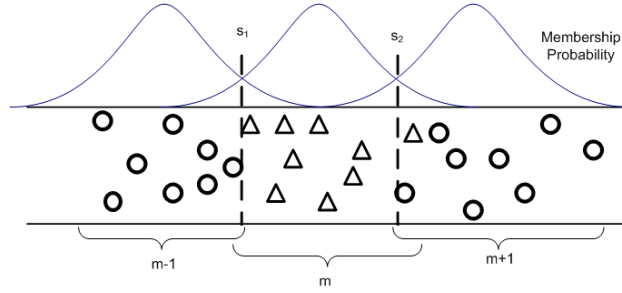


Figure 3.2: Formation of levels along with membership probability.

subsequent levels are formed until the destination is reached or the message is broadcasted to the entire network. It can be noticed that during the entire transmission process, a hop is formed opportunistically and that there are no fixed boundaries between the nodes of two levels as shown in Fig. 3.2.

Let ϕ denotes a stationary Poisson point process (PPP) on a hop with intensity $\tilde{\lambda}$ such that the average number of nodes in a level is $\tilde{\gamma} = \tilde{\lambda}|S|$, where $|S|$ denotes the span of a single level. The probability of having k_n nodes in one level is thus given by

$$\mathbb{P}(\phi(S) = k_n) = \exp(-\tilde{\lambda}|S|) \frac{(\tilde{\lambda}|S|)^{k_n}}{k_n!}. \quad (3.1)$$

In a realistic scenarios, each level or hop contains a random number of nodes and the message is broadcasted or unicasted using cooperative transmission (CT). The number of hops required to deliver a message to a given distance is dependent upon the network parameters. The PPP is a suitable approximation as it allows to model the random number of nodes per level as compared

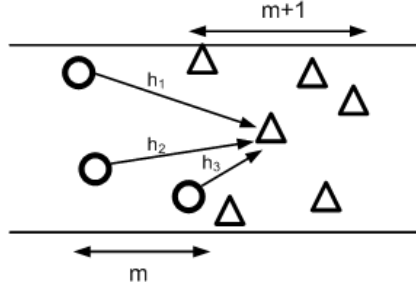


Figure 3.3: Transmission of signal from one hop to another without a fixed hypothetical boundary. A single node constitutes a MISO scenario.

to a fixed number of nodes per hop modeled generally with a binomial point process.

The multiple copies of the same signal received by a node, transmitted by a group of nodes in the previous level, are assumed to be synchronous over independent fading channels [17] and are transmitted with equal transmit power. A virtual multiple-input single-output (MISO) is formed as shown in Fig. 3.3, which gives rise to spatial diversity and hence more reliability. A hop is said to be successful, if there exists at least one DF node in the next hop provided the DF nodes in the previous level relayed the signal. The intensity of the DF nodes in level m is $\lambda = \tilde{\lambda} P_s^m$ [42], where P_s is the success probability of a node. The intensity of the DF nodes is reduced, however, they still follow a PPP. In one CT session, a node can only transmit once, however a node may receive and successfully decode the same signal multiple times. Since a node cannot forward the same signal multiple times, hence it will be a part of only one group of DF nodes in one level. However in subsequent CT sessions, a node can be a part of different group of DF nodes or levels, hence the membership of a node to a particular level becomes random.

3.2 Membership of a Node

The tendency of the nodes to be in the same hop or level in subsequent iterations of the CT is higher for the nodes present around the center of a level and decreases gradually for the nodes located near the boundary. Nodes can transmit the signal once and can become a member of only one hop. The membership probability of a node that it transmits in hop m is different for every other node of the hop as shown in Fig. 3.2. For instance, a node located near the boundary of hop, $m - 1$, can become a member of the next hop, m , provided it has not transmitted the signal before and successfully decoded the signal in next time slot. The nodes located at point s_1 have almost equal probability of becoming a member of hop $m - 1$ or m . Hence a straight forward way is that the membership probability is modeled with a normal distribution with some mean and variance. The length of the hop or level controls the variance and mean is dependent upon the center of the hop. We will show later that our assumption for the membership function to be Gaussian is correct

3.3 Received Power

Let $\phi(S_m)$ denotes the number of DF nodes at a level m , then the received power at any node j at level $m + 1$ is given as

$$P_{r_j}(m + 1) = \sum_{i \in \phi(S_m)} \frac{P_t h_{ij}}{d_{ij}^\alpha}, \quad (3.2)$$

where P_t represents the transmitted power, h_{ij} denotes the effects of Rayleigh flat fading modeled with the unit mean exponential RV, d is the Euclidean distance between node i and j of two different levels and α is the path loss exponent.

Chapter 4

SISO Links

In this chapter, we derive the distribution of the received power for SISO links. In SISO links, the communication between two random nodes is shown in Fig. 4.1. The received signal will be forwarded to the next node if the received signal power is greater than a predefined decoding threshold, τ . The received power while considering only two channel distortions, fading

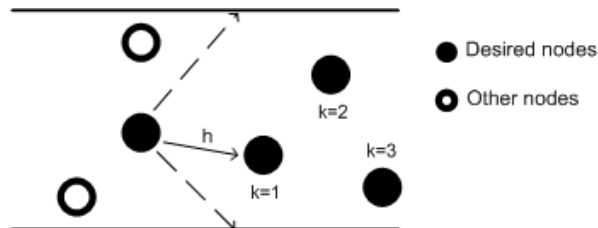


Figure 4.1: Transmission of signal from one node to another without fixed boundary

and path loss, is given by

$$P_r = \frac{P_t h}{d^\alpha}, \quad (4.1)$$

where P_t is the transmit power, h characterizes the phenomenon of fading, d represents the Euclidean distance between the transmitter and the receiver

and α is the path loss exponent. The RV H is drawn from an exponential distribution, which models the squared envelope of the signal experiencing Rayleigh fading. The probability density functions (PDF) of H is given by

$$f_H(h) = \omega \exp(-\omega h), \quad (4.2)$$

where ω is the mean of the exponential distribution. The distance, d , to the k th nearest neighbor is modeled by a GG RV [31], V , and its PDF is given by

$$f_V(v) = \frac{\epsilon}{\Gamma(k) \delta^{k\epsilon}} v^{k\epsilon-1} \exp\left\{-\left(\frac{v}{\delta}\right)^\epsilon\right\}, \quad (4.3)$$

where $\epsilon = 2$ characterizes a 2D network and $\Gamma(\cdot)$ is the gamma function. In the above equation, $\delta = (\bar{\lambda} c_{\vartheta, \epsilon})^{-1/\epsilon}$ and $c_{\vartheta, \epsilon}$ is the parameter which determines the angular range where the next neighboring node lies, where $\bar{\lambda}$ is the intensity of the nodes in the strip shaped network. For efficient transmission, the next hop node should be nearer to the destination, i.e., the next hop node should lie within the specified angle $0 < \vartheta < \frac{\pi}{2}$ as reference to the source-destination vector. Usually $c_{\vartheta, \epsilon} = \pi/4$ for neighboring node to exist within 90° sector as shown in Fig. 4.1 with dotted lines. There may be many neighboring nodes to be part of next hop and the value of k determines that specific node with which the SISO link should be established. If $k = 1$, then node communicates with the first nearest neighbor. Whereas, when $k = 2$, the transmitting node communicates with the second nearest neighbor as shown in Fig. 4.1, while the distance is distributed according to (4.3), the distribution of the distance raised to power, α , where $d^\alpha \in F$ and $F = V^\alpha$ is given as

$$f_F(f) = \frac{1}{\alpha} f^{\frac{1}{\alpha}-1} f_V(f^{\frac{1}{\alpha}}). \quad (4.4)$$

Using (4.3) and (4.4), the distribution of the distance raised to power, α ,

is given by

$$f_F(f) = \frac{\beta}{\Gamma(k)\theta^{k\beta}} f^{k\beta-1} \exp\left\{-\left(\frac{f}{\theta}\right)^\beta\right\}, \quad (4.5)$$

where $\beta = \epsilon/\alpha$ and $\theta = \delta^\alpha$.

It can be observed from (4.1) that the coverage probability of the receiving node, P_s , is a doubly stochastic process that depends upon two RVs. For coverage probability, the cumulative distribution function CDF of the received power is required to be calculated and the received power in (4.1) is the ratio of two RVs, i.e., exponential RV H and GG RV F . The ratio distribution of an exponential RV and GG RV is derived in the next section.

4.1 Ratio of an exponential RV and GG RV

The CDF of the ratio in (4.1) is expressed in the following theorem.

Theorem 1. *The CDF of $Z = H/Y$, where H and F are distributed according to (4.2) and (4.5) respectively, is given by*

$$F_Z(z) = \frac{\beta}{\Gamma(k)\theta^{k\beta}} \left[\frac{\Gamma(k)}{\beta\theta^{-\beta k}} - \frac{\Gamma(k\beta)}{z^{k\beta}} + \frac{\beta}{z^{k\beta}\theta^\beta} \left\{ \frac{(\omega z)^{-\beta}}{\beta} \times \right. \right. \quad (4.6)$$

$$\left. \left. \sum_{n=0}^{\infty} \frac{\Gamma(k\beta + \beta + n\beta)}{(n+1)!} \left(\frac{-1}{(z\theta\omega)^\beta} \right)^n \right\} \right]$$

for $\beta < 1$,

$$F_Z(z) = \frac{\beta}{\Gamma(k)\theta^{k\beta}} \left[\frac{\Gamma(k)}{\beta\theta^{-\beta k}} - \frac{\beta\omega^{k\beta}\Gamma(k\beta)\theta^{1+k\beta}}{\theta^\beta(1+\omega z\theta)^{k\beta}} \right] \quad (4.7)$$

for $\beta = 1$,

$$F_Z(z) = \frac{\beta}{\Gamma(k) \theta^{k\beta}} \left[\frac{\Gamma(k)}{\beta \theta^{-\beta k}} - (\omega)^{k\beta} \theta^{k\beta} \right. \quad (4.8)$$

$$\left. \times \left\{ \sum_{n=0}^{\infty} \frac{1}{n! (n + k\beta)} \Gamma\left(\frac{k\beta + \beta + n}{\beta}\right) (-\omega z \theta)^n \right\} \right]$$

for $\beta > 1$.

Proof. The CDF of Z involves the CDF of H given by

$$F_H(h) = 1 - \exp(-\omega h). \quad (4.9)$$

Using (4.5) and (4.9), the CDF of Z can be calculated as

$$\mathbb{P}(Z \leq z) = \int_0^{\infty} F_H(zf) f_F(f) df \quad (4.10)$$

$$= \frac{\beta}{\Gamma(k) \theta^{k\beta}} \int_0^{\infty} (1 - e^{-\omega z f}) f^{k\beta-1} e^{-\left(\frac{f}{\theta}\right)^\beta} df \quad (4.11)$$

$$= \frac{\beta}{\Gamma(k) \theta^{k\beta}} \left[\int_0^{\infty} f^{k\beta-1} e^{-\left(\frac{f}{\theta}\right)^\beta} df - \right. \quad (4.12)$$

$$\left. \int_0^{\infty} e^{-\omega z f} f^{k\beta-1} e^{-\left(\frac{f}{\theta}\right)^\beta} df \right] \quad (4.13)$$

Solving the first integral directly and applying integration by parts on the second integral, we get

$$\mathbb{P}(Z \leq z) = \frac{\beta}{\Gamma(k) \theta^{k\beta}} \left\{ \frac{\Gamma(k)}{\beta \theta^{-k\beta}} - \left[-e^{-\left(\frac{f}{\theta}\right)^\beta} \frac{\Gamma(k\beta, \omega z f)}{z^{k\beta}} \right]_0^{\infty} + \right. \quad (4.14)$$

$$\left. \int_0^{\infty} \frac{\beta \Gamma(k\beta, \omega z f) e^{-\left(\frac{f}{\theta}\right)^\beta} f^{\beta-1}}{z^{k\beta} \theta^\beta} df \right\}.$$

Simplifying the above, the CDF of Z becomes

$$\mathbb{P}(Z \leq z) = \frac{\beta}{\Gamma(k) \theta^{k\beta}} \left\{ \frac{\Gamma(k)}{\beta \theta^{-k\beta}} - \frac{\Gamma(k\beta)}{z^{k\beta}} + \right. \quad (4.15)$$

$$\left. \frac{\beta}{z^{k\beta} \theta^\beta} \int_0^\infty \Gamma(k\beta, \omega z f) e^{-\left(\frac{f}{\theta}\right)^\beta} f^{\beta-1} df \right\}$$

$$= \frac{\beta}{\Gamma(k) \theta^{k\beta}} \left\{ \frac{\Gamma(k)}{\beta \theta^{-k\beta}} - \frac{\Gamma(k\beta)}{z^{k\beta}} + \frac{\beta}{z^{k\beta} \theta^\beta} I \right\}. \quad (4.16)$$

Integral I in (4.16) is prohibitive to compute for all values of β simultaneously as it involves three types of functions, i.e., incomplete gamma function, a power function and an exponential function. To reduce the complexity of the integral and to get a closed-form, we split the variable β and solve three slightly different integrals. The conditional integral computation, conditioned on value of β is given as

$$I = \begin{cases} \frac{(\omega z)^{-\beta}}{\beta} \sum_{n=0}^{\infty} \frac{\Gamma(k\beta + \beta + n\beta)}{(n+1)!} \left(\frac{-1}{(z\theta\omega)^\beta} \right)^n, & \text{if } \beta < 1, \\ \theta \Gamma(k\beta) - (\omega z)^{k\beta} \Gamma(k\beta) \theta^{1+k\beta} \\ \times {}_2F_1(k\beta, k\beta + 1; k\beta + 1; -\omega z \theta), & \text{if } \beta = 1, \\ \frac{\Gamma(k\beta) \theta^\beta}{\beta} - (\omega z)^{k\beta} \theta^{\beta(k+1)} \\ \times \sum_{n=0}^{\infty} \frac{(-\omega z \theta)^n}{n! (n + k\beta)} \Gamma\left(\frac{k\beta + \beta + n}{\beta}\right), & \text{if } \beta > 1. \end{cases} \quad (4.17)$$

The hypergeometric term in (4.17) can be simplified as

$${}_2F_1(k\beta, k\beta + 1; k\beta + 1; -\omega z \theta) = (1 + \omega z \theta)^{-k\beta}. \quad (4.18)$$

Putting the values of I back in (4.16) provides (4.6)-(4.8), respectively and thus completes the proof. ■

4.2 Coverage Probability

The ratio distribution derived above is actually the distribution of the received power and using the ratio distribution, the coverage probability at a node can be derived. The coverage probability is given by

$$P_s = \mathbb{P}(P_r \geq \tau) = 1 - \mathbb{P}(P_r \leq \tau) = 1 - P_o, \quad (4.19)$$

where P_o is the outage probability. The outage probability at a node is derived by evaluating the CDF of the ratio at $F_Z(\tau/P_t)$ and is given by

$$P_o = \frac{\beta}{\Gamma(k)\theta^{k\beta}} \left[\frac{\Gamma(k)}{\beta\theta^{-\beta k}} - \frac{\Gamma(k\beta)}{(\tau/P_t)^{k\beta}} + \frac{\beta}{(\tau/P_t)^{k\beta}\theta^\beta} \times \right. \quad (4.20)$$

$$\left. \left\{ \frac{(\omega\tau/P_t)^{-\beta}}{\beta} \sum_{n=0}^{\infty} \frac{\Gamma(k\beta + \beta + n\beta)}{(n+1)!} \left(\frac{-1}{(\theta\omega\tau/P_t)^\beta} \right)^n \right\} \right]$$

for $\beta < 1$,

$$P_o = \frac{\beta}{\Gamma(k)\theta^{k\beta}} \left[\frac{\Gamma(k)}{\beta\theta^{-\beta k}} - \frac{\beta\omega^{k\beta}\Gamma(k\beta)\theta^{1+k\beta}}{\theta^\beta(1+\omega\theta\tau/P_t)^{k\beta}} \right] \quad (4.21)$$

for $\beta = 1$,

$$P_o = \frac{\beta}{\Gamma(k)\theta^{k\beta}} \left[\frac{\Gamma(k)}{\beta\theta^{-\beta k}} - (\omega)^{k\beta}\theta^{k\beta} \right. \quad (4.22)$$

$$\left. \times \left\{ \sum_{n=0}^{\infty} \frac{1}{n!(n+k\beta)} \Gamma\left(\frac{k\beta + \beta + n}{\beta}\right) (-\omega\theta\tau/P_t)^n \right\} \right]$$

for $\beta > 1$.

Chapter 5

Virtual MISO Links

In this chapter, we derive the distribution of the received power for virtual MISO links. For simplification purpose, we first consider a random strip-shaped network with hypothetical boundaries as shown in Fig. 5.1 and then extend our analysis for irregular hop boundaries.

5.1 Virtual MISO links with Hypothetical Boundaries

The network in Fig. 5.1 is divided into hypothetical boundaries, which form multiple levels of square shape of $L \times L$. The GG distribution does not remain a valid distance distribution between a pair of nodes in adjacent levels, as GG distribution cannot differentiate between the nodes of the same level or adjacent level. Therefore, the received power is calculated using (3.2), where d_{ij}^α can be approximated as a Weibull RV with shape parameter $c = 3.1612/\alpha$ and scale parameter $\chi = (4L^2/3\Gamma(1.6327))^{\alpha/2}$ [28] and $\Gamma(\cdot)$ is an incomplete gamma function.

The received power for the virtual MISO network as shown in Fig. 3.3,

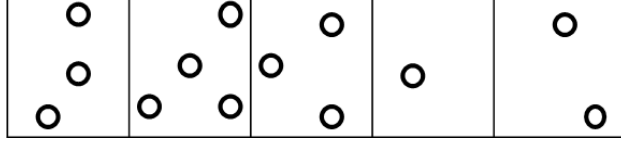


Figure 5.1: A strip-shaped network with hypothetical boundaries and random node locations.

is the sum of ratio of an exponential RV, H , and a Weibull RV, Q , where the sum is dependent upon the number of the DF nodes in the previous level which are distributed according to a PPP. As in (3.2), the received power is given as

$$P_{r_j}(m+1) = P_t \sum_{i \in \phi(S_m)} \frac{H_i}{Q_i} \triangleq P_t \sum_{i \in \phi(S_m)} R_i, \quad (5.1)$$

where $\phi(S_m)$ is the number of the DF nodes in level m . To study such networks, the PDF of the received power needs to be determine by self-convolving the distribution of RVs R_i as they are independent and identically distributed (I.I.D). The PDF of a single RV, R , is given as [33]

$$f_R(r) = \chi \sum_{n=0}^{\infty} \frac{1}{n!} \Gamma\left(\frac{1+c+n}{c}\right) (-r\chi)^n. \quad (5.2)$$

We consider the following theorem for finding the coverage probability of a virtual MISO link.

Theorem 2 (Outage Probability of a virtual MISO link). *If nodes in each level are distributed according to a PPP with mean $\tilde{\gamma} = \tilde{\lambda}|S|$ and the mean of the DF nodes in the previous level n is $\gamma = \lambda|S|$, then the outage probability, P_o , for a random node in the next level $n+1$ is given by*

$$P_o = \exp(-\gamma) \left[\sum_{m=0}^{\infty} \frac{(\gamma\chi)^m}{m!} \sum_{a_1=0}^{\infty} \sum_{a_2=0}^{\infty} \dots \right. \quad (5.3)$$

$$\left. \sum_{a_m=0}^{\infty} \frac{(\tau/P_t)^{a_1+a_2+\dots+a_m+m}}{(a_1+a_2+\dots+a_m+m)!} \prod_{i=1}^m \Gamma\left(\frac{1+c+a_i}{c}\right) (-\chi)^{a_i} \right].$$

Proof. The self-convolution of the distribution of the ratio RVs, R , is reduced to their product in frequency domain, given as

$$\mathcal{L} \left[*_{z=1}^{k_n} f_{R_z}(r_z) \right] = \prod_{z=1}^{k_n} F_z(s) = (F(s))^{k_n}, \quad (5.4)$$

where $*$ denotes the convolution operator, \mathcal{L} is the Laplace operator and $F(s)$ is the Laplace transform of $f_R(r)$, given as

$$F(s) = \chi \sum_{n=0}^{\infty} \frac{1}{n!} \Gamma\left(\frac{1+c+n}{c}\right) (-\chi)^n \frac{1}{s^{n+1}}. \quad (5.5)$$

The value of RV, k_n , in (5.4) depends upon the number of nodes in the previous level. We calculate the expected value of $(F(s))^{k_n}$ with respect to the Poisson RV, k_n , with mean $\gamma = \lambda|S|$ as

$$\begin{aligned} G(s) &= \mathbb{E} \left[(F(s))^{k_n} \right] \\ &= \sum_{k_n=0}^{\infty} \frac{(\lambda|S|)^{k_n} \exp(-\lambda|S|)}{k_n!} (F(s))^{k_n}. \end{aligned} \quad (5.6)$$

After some mathematical manipulation, we obtain

$$G(s) = \exp \left(\lambda|S| \chi \sum_{n=0}^{\infty} \frac{1}{n!} \Gamma\left(\frac{1+c+n}{c}\right) (-\chi)^n \frac{1}{s^{n+1}} \right) \exp(-\lambda|S|). \quad (5.7)$$

The above function is quite complex and direct inverse Laplace transform is prohibited in closed-form, so we expand the first exponential function in (5.7) with a Taylor series such that

$$G(s) = \sum_{m=0}^{\infty} \left(\lambda|S| \chi \sum_{n=0}^{\infty} \frac{1}{n!} \Gamma\left(\frac{1+c+n}{c}\right) (-\chi)^n \frac{1}{s^{n+1}} \right)^m \exp(-\lambda|S|). \quad (5.8)$$

Simplifying the above function for m , we get

$$G(s) = \left[\sum_{m=0}^{\infty} \frac{(\lambda S \chi)^m}{m!} \sum_{a_1=0}^{\infty} \cdots \sum_{a_m=0}^{\infty} \frac{1}{s^{a_1+a_2+\dots+a_m+m}} \prod_{i=1}^m \Gamma\left(\frac{1+c+a_i}{c}\right) (-\chi)^{a_i} \right] \exp(-\lambda|S|). \quad (5.9)$$

The PDF of the receive power, P_r , is found by taking the inverse Laplace transform of the $G(s)$, given as

$$f_{P_r}(p_r) = \exp(-\lambda|S|) \left[\sum_{m=0}^{\infty} \frac{(\lambda|S|\chi)^m}{m!} \sum_{a_1=0}^{\infty} \sum_{a_2=0}^{\infty} \cdots \sum_{a_m=0}^{\infty} \right. \quad (5.10)$$

$$\left. \frac{(p_r)^{a_1+a_2+\dots+a_m+m-1}}{(a_1+a_2+\dots+a_m+m-1)!} \prod_{i=1}^m \Gamma\left(\frac{1+c+a_i}{c}\right) (-\chi)^{a_i} \right].$$

The integration of the above expression will yield the CDF, $F_{P_r}(p_r)$, of the received power and outage probability, P_o , is obtained by evaluating the CDF at $F_{P_r}(\tau/P_t)$. ■

The coverage probability is calculated using (5.3), such that

$$P_s = \mathbb{P}(P_r \geq \tau) = 1 - \mathbb{P}(P_r \leq \tau) = 1 - P_o. \quad (5.11)$$

5.2 Distance Distribution between a pair of nodes without any Hypothetical Boundary

Removing the constraint of the hypothetical boundaries changes the distance distribution. A new distance distribution needs to be derived between the

pair of nodes. In this section, we derive the distribution of the random distance between a pair of nodes in adjacent levels. As shown in Fig. 3.1, the network has a fixed vertical length and extends in the horizontal dimension. The nodes are distributed uniformly in the 2D network in both directions but the formation of levels changes the node distribution in horizontal direction with respect to a level or hop. The membership of nodes provides us important information about the distribution of nodes comprising in one level. Nodes in the horizontal direction are concentrated around the center of the level and stretches in the outward direction, whereas nodes are uniformly distributed in the vertical direction. The candidate node locations within one of the levels is modeled with a random variables (RV). The horizontal component is modeled with normal RV X given by

$$f_X(x) = \frac{1}{\sigma\sqrt{2\pi}} \exp\left(-\frac{(x-\nu)^2}{2\sigma^2}\right), \quad (5.12)$$

where ν is the mean of the normal distribution representing the center of a level and σ is the standard deviation characterizing the size of the level. On the other hand, uniform distribution is used to model the vertical component, given by

$$f_Y(y) = \begin{cases} \frac{1}{B}, & \text{if } 0 \leq y \leq B, \\ 0, & \text{otherwise,} \end{cases} \quad (5.13)$$

where B is the width of the strip-shaped network. These two RVs completely describe the location of a node in one level. Let $A_1(x_1, y_1)$ and $A_2(x_2, y_2)$ be the two random nodes in adjacent levels at positions $x_i, y_i; i \in \{1, 2\}$ as shown in Fig. 5.2, then the Euclidean distance between two nodes is given by

$$d = \sqrt{(x_2 - x_1)^2 + (y_2 - y_1)^2}. \quad (5.14)$$

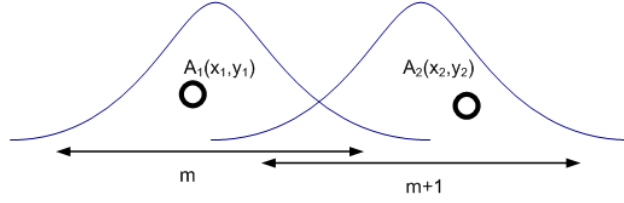


Figure 5.2: A realization of a pair of nodes placed randomly in adjacent levels.

In (5.14), $x_i \in X_i$ and $y_i \in Y_i \forall i = \{1, 2\}$, where $X_i \sim N(\nu_i, \sigma_i^2)$ and $Y_i \sim U[0, B]$. If the means and variances of X_1 and X_2 are (ν_1, σ_1^2) and (ν_2, σ_2^2) respectively, then the difference between two normal RVs $X_2 - X_1$ is also a normal RV O , whose PDF is given as

$$f_O(o) = \frac{1}{\Delta\sqrt{2\pi}} \exp\left(-\frac{(o - \mu)^2}{2\Delta^2}\right), \quad (5.15)$$

where $\mu = \nu_2 - \nu_1$ with standard deviation $\Delta = \sqrt{\sigma_1^2 + \sigma_2^2}$. However from (5.14), the squared difference of RVs, i.e., $(X_2 - X_1)^2$ is desired, which for normal RVs is given as a non-central chi-squared RV. Limiting this distribution to one degree freedom will provide the distribution of the squared normal RV, $T = O^2$, given as

$$f_T(t) = \frac{1}{2\sqrt{2\pi}\Delta^2 t} \exp\left(-\frac{t + \mu^2}{2\Delta^2}\right) \times \left[\exp\left(\sqrt{\frac{\mu^2 t}{\Delta^4}}\right) + \exp\left(-\sqrt{\frac{\mu^2 t}{\Delta^4}}\right) \right], \quad t \geq 0. \quad (5.16)$$

Similarly, for the y -component, let $P = Y_2 - Y_1$ and its probability density function (PDF) is given as

$$f_P(p) = \begin{cases} \frac{1}{B^2} (B + p), & \text{if } -B < p \leq 0, \\ \frac{1}{B^2} (B - p), & \text{if } 0 < p \leq B, \\ 0, & \text{otherwise.} \end{cases} \quad (5.17)$$

The distribution of $L = P^2$ is then given as [43]

$$f_L(l) = \begin{cases} \frac{1}{B\sqrt{l}} - \frac{1}{B^2}, & \text{if } 0 < l \leq B^2, \\ 0, & \text{otherwise.} \end{cases} \quad (5.18)$$

The distribution of the squared Euclidean distance is thus equal to the distribution of the sum of RVs T and L , having distributions given in (5.16) and (5.18), respectively. However, this addition of RVs is not straight forward owing to the non linear terms in (5.18). Hence the distribution of RV L is approximated with another distribution, complying with the features of L as shown in the following Lemma.

Lemma 1. *The distribution of the square of the difference between two uniform RVs can be approximated by a central chi-squared distribution with variance, $v = 0.408B$, given as*

$$f_G(g) = \frac{1}{\sqrt{2\pi v^2 g}} \exp\left(-\frac{g}{2v^2}\right), \quad g \geq 0. \quad (5.19)$$

Proof. Central chi-squared distribution closely matches the distribution of L , with one degree of freedom, using moments matching method. It models the squared sum of zero mean normal RVs. Since the distribution of L involves only one parameter, so matching only the first moment is enough. The first moment of L is calculated as

$$\mathbb{E}[L] = \int_0^{W^2} l f_L(l) dl = \frac{B^2}{6}, \quad (5.20)$$

where $\mathbb{E}[\cdot]$ is the expected value. The expected value of central chi-squared RV, G , with one degree of freedom is calculated as

$$\mathbb{E}[G] = 2v^2 \frac{\Gamma(1 + 1/2)}{\sqrt{\pi}}, \quad (5.21)$$

where v is the standard deviation of the zero mean normal RV and $\Gamma(\cdot)$ is the gamma function. Matching the moments and solving the equation will provide the value of v depending upon the width, B , of the strip-shaped network, given as

$$v = 0.408B. \quad (5.22)$$

Hence the new distribution for RV L approximated with RV G is given in (5.19). ■

The squared Euclidean distance now becomes the sum of a non-central chi-squared RV from (5.16) and a central chi-squared RV from (5.19), for which we define $N = T + G$. Note that T and G are independent RVs and the distribution of their sum is given as [44]

$$f_N(n) = \frac{1}{2\Delta v} \exp\left(-\frac{n + \mu^2}{2\Delta^2}\right) \sum_{i=0}^{\infty} \frac{\Gamma(1/2 + i)}{i! \Gamma(1/2)} \times \quad (5.23)$$

$$\left(\frac{\sqrt{n}(v^2 - \Delta^2)}{\mu v^2}\right)^i I_i\left(\frac{\sqrt{n}\mu}{\Delta^2}\right), \quad n \geq 0,$$

where $\Gamma(\cdot)$ denotes the gamma function and $I_i(\cdot)$ is the modified Bessel function of the first kind.

To find the distribution of the received power using the distance distribution derived above becomes prohibitive as (5.23) involves infinite summation terms. Therefore, to analytically derive a closed-form expression for the PDF of received power, we need to approximate (5.23) with some tractable expression. Using the moments matching method, we approximate the squared

distance distribution to another function with similar properties and complying with the effects of the parameters μ , Δ and v of RV N , as shown in the following Lemma.

Lemma 2. *The distribution of the Euclidean distance between a pair of nodes in two adjacent levels as shown in Fig. 5.2, can be approximated by a Weibull distribution with shape parameter, c , and scale parameter, χ , such that*

$$f_Q(q) = \frac{c}{\chi^c} q^{c-1} \exp \left[- \left(\frac{q}{\chi} \right)^c \right], \quad q \geq 0, \quad (5.24)$$

where $\chi = \zeta^{\alpha/2}$, $c = 2\kappa/\alpha$ and the values of ζ and κ are given in (5.28)

Proof. The moments matching method is used to show that the Weibull distribution closely matches the squared distance distribution, N . It is a two parameter distribution, i.e., shape parameter, κ , and scale parameter, ζ . The first moment of N is calculated as

$$\mathbb{E}[N] = \int_0^\infty n f_N(n) dn = \mu^2 + \Delta^2 + v^2. \quad (5.25)$$

and the second moment is

$$\begin{aligned} \mathbb{E}[N^2] &= \int_0^\infty n^2 f_N(n) dn \\ &= \mu^4 + 3\Delta^4 + 3v^4 + 2\Delta^2 v^2 + 2\mu^2 (v^2 + 3\Delta^2). \end{aligned} \quad (5.26)$$

The first two moments of Weibull RV, W , are

$$\begin{aligned} \mathbb{E}[W] &= \zeta \Gamma \left(1 + \frac{1}{\kappa} \right), \\ \mathbb{E}[W^2] &= \zeta^2 \Gamma \left(1 + \frac{2}{\kappa} \right). \end{aligned} \quad (5.27)$$

Proceeding with the algorithm of moments matching, we get two non-linear equations. Simplifying the equations we get

$$\begin{aligned} \zeta &= \frac{\mu^2 + \Delta^2 + v^2}{\Gamma(1 + 1/\kappa)}, \\ \frac{\Gamma(1 + 2/\kappa)}{[\Gamma(1 + 1/\kappa)]^2} &= 1 + \frac{4\mu^2 \Delta^2 + 2\Delta^2 + 2v^2}{(\mu^2 + \Delta^2 + v^2)^2}. \end{aligned} \quad (5.28)$$

The value of ζ is dependent upon the value of κ , whereas the value of κ is calculated numerically. Hence the new distribution of the squared Euclidean distance is given as

$$f_W(w) = \frac{\kappa}{\zeta^\kappa} w^{\kappa-1} \exp \left[- \left(\frac{w}{\zeta} \right)^\kappa \right], \quad w \geq 0. \quad (5.29)$$

In (3.2), distance is raised to path loss exponent, α , so the distribution of the distance raised to power, α , where $d^\alpha \in Q$ and $Q = W^{\alpha/2}$, is calculated using (4.4). Hence the distribution of the Euclidean distance raised to power, α , for the network shown in Fig. 5.2, is also Weibull given in (5.24). ■

5.3 Virtual MISO Links with Irregular Hop Boundaries

The received power for a virtual MISO links with irregular hop boundaries as shown in Fig. 3.3 are calculated using the expressions derived in Section 5.1 and the distance distribution derived in the previous section. The coverage probability is calculated using Theorem 2 and (5.11).

The coverage probability is inversely proportional to χ , which specifies the distance distribution and directly proportional to the node intensity. The coverage probability, P_s , is same for each node of any one level. The one-hop success probability, P_{one} , is calculated using the coverage probability, given as

$$P_{one} = \mathbb{P}(k_n \geq 1) = 1 - \mathbb{P}(k_n = 0) = 1 - \exp(-\lambda|S|P_s). \quad (5.30)$$

Chapter 6

Energy Efficiency

The energy efficiency of the system can be improved by limiting the number of nodes per level that relay the information. Usually for a network with a high node density, the transmissions from all the DF nodes of one level are not required for the formation of the next level. Similar results can be achieved by having a limited node participation at different hops. The nodes present near the source or the boundary of previous level have much higher received powers owing to less average path loss and when they transmit to the next level nodes, their transmissions have little or no effect on the decoding of the nodes of next level because of large path loss between them and the next level nodes. Limiting such nodes from transmission to the next level and allowing only those nodes which are nearer to the next level boundary, conserves a significant amount of energy. Hence in this section, we devise a method to improve the energy efficiency of the network by having limited node participation.

The nodes in one level are divided into two subsets of transmitters based on the above criteria, i.e., effective transmitters and futile transmitters as shown in Fig. 6.1. The two subsets of the transmitters do not need to

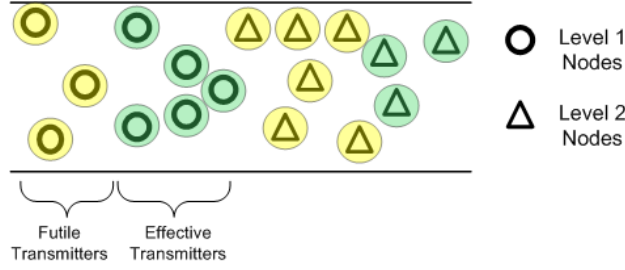


Figure 6.1: Two subsets of transmitters.

be of equal sizes. Their sizes can vary, however, increasing the number of nodes in one subset decreases the number of nodes in the other and vice versa. The size of two subsets can be made dependent upon the quality of service (QoS), η , and other network parameters. The QoS in this case can be defined as the minimum end-to-end success probability required for the network. We devise the thinning of OLA (Th-OLA) algorithm, which is derived from the basic OLA with additional constraint for transmission that the nodes must be closer to the boundary of the next level. This type of situation can be attributed to a larger rectangular area, where nodes are distributed according to a PPP, but for transmission purpose, only the nodes of a smaller rectangular area are selected as shown in Fig. 6.2. We consider the following the theorem for the thinning of PPP.

Theorem 3. *If nodes are distributed according to a PPP, ϕ , with intensity λ in an area $|S|$ and the thinning function permits only j nodes located in the area $|D|$, where $|D| \subseteq |S|$ almost surely, then the distribution of the nodes in area $|D|$ still follows another PPP, $\bar{\phi}$, with same intensity λ , such that*

$$\mathbb{P}(\bar{\phi}(D) = j) = \exp(-\lambda|D|) \frac{(\lambda|D|)^j}{j!}. \quad (6.1)$$

Proof. Let $\phi(S)$ be the PPP with mean $\lambda|S|$ and $\bar{\Phi}(D)$ be the process ob-

tained after thinning. The distribution of $\bar{\phi}(D)$ can be calculated as

$$\mathbb{P}(\bar{\phi}(D) = j) = \sum_{k_n=j}^{\infty} \mathbb{P}(\phi(S) = k_n) \mathbb{P}(\bar{\phi}(D) = j | \phi(S) = k_n), \quad (6.2)$$

where k_n is the number of the nodes in the original PPP and j denotes the number of nodes in the new process obtained after thinning. Since the nodes are distributed uniformly, we calculate the conditional probability of finding a node in $\bar{\phi}(D)$ given that $\phi(S) = 1$ as

$$\mathbb{P}(\bar{\phi}(D) = 1 | \phi(S) = 1) = \frac{|D|}{|S|}. \quad (6.3)$$

The conditional probability of $\bar{\phi}(D) = j$ given that $\phi(S) = k_n$ is given as

$$\mathbb{P}(\bar{\phi}(D) = j | \phi(S) = k_n) = \binom{k_n}{j} \left(\frac{|D|}{|S|} \right)^j \left(1 - \frac{|D|}{|S|} \right)^{k_n-j}. \quad (6.4)$$

Using the above expression in (6.2), we get

$$\mathbb{P}(\bar{\phi}(D) = j) = \sum_{k_n=j}^{\infty} \exp(-\lambda|S|) \frac{(\lambda|S|)^{k_n}}{k_n!} \times \quad (6.5)$$

$$\binom{k_n}{j} \left(\frac{|D|}{|S|} \right)^j \left(1 - \frac{|D|}{|S|} \right)^{k_n-j} \\ = \exp(-\lambda|S|) \frac{(\lambda|D|)^j}{j!} \times \quad (6.6)$$

$$\sum_{k_n=j}^{\infty} \frac{[\lambda|S|(1 - |S|^{-1}|D|)]^{k_n-j}}{(k_n - j)!}.$$

After some mathematical manipulations, we obtain

$$\mathbb{P}(\bar{\phi}(D) = j) = \exp(-\lambda|S|) \frac{(\lambda|D|)^j}{j!} \times \\ \exp[\lambda|S|(1 - |S|^{-1}|D|)] \quad (6.7) \\ = \frac{(\lambda|D|)^j}{j!} \exp(-\lambda|D|).$$

Hence the thinning process directly reduces the effective hop area, whereas the intensity of the nodes remains the same with same distribution. ■

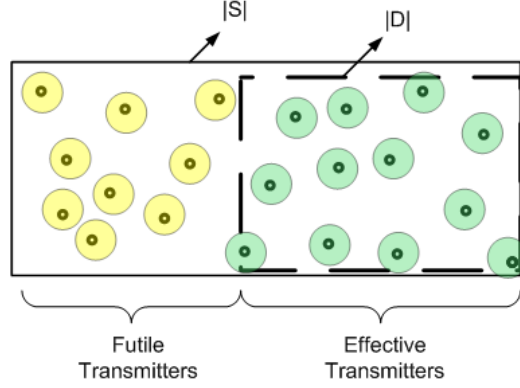


Figure 6.2: Thinning of PPP.

The distance between the nodes of two consecutive hops is modeled with (5.24) with reduced mean, $\tilde{\mu}$, and reduced standard deviation, $\tilde{\Delta}$, as the effective transmit area of a hop reduces, however, Theorem 2 can be used to analyze the Th-OLA. The value of $\tilde{\mu}$ is always less than μ as the effective hop area cannot be greater than the original one.

Let the number of the nodes that relay the signal at level i is $k_{n,i}$ in basic OLA and the number of the nodes that relay the signal after thinning process is j_i . Then the total transmit power for basic OLA in transmitting the signal up to m hops while maintaining a QoS is $P_t \sum_{i=0}^m k_{n,i}$, which is dependent upon the RV k_n and the ergodic mean of the total energy consumed is $P_t m \gamma_b$, where γ_b is the average number of nodes per hop for basic OLA. Similarly, the total transmit energy for thinned OLA is $P_t \sum_{i=0}^m j_i$ and its mean value is $P_t m \gamma_t$, where γ_t is the average number of nodes per hop for Th-OLA. The

fraction of energy saved (FES) can be calculated as

$$\begin{aligned} FES &= 1 - \frac{\text{Total energy of the Th-OLA}}{\text{Total energy of the basic OLA}} \\ FES &= 1 - \frac{P_t m \gamma_t}{P_t m \gamma_b} \\ &= 1 - \frac{\gamma_t}{\gamma_b}. \end{aligned} \tag{6.8}$$

Chapter 7

Results and Discussions

7.1 SISO Links

In this section, we validate the analytical results along with the performance characterization of the SISO network in terms of coverage probability, hop count and energy conservation. The analytical expressions derived in the theorem 1 are verified by comparing it with Monte-Carlo simulations. For simulation purpose, exponential and generalized gamma RVs are generated and their ratio is calculated using (4.1). This process is repeated over $1e^5$ iterations and the CDF is calculated. The value of path loss exponent, α , controls the value of β as shown in (4.5). The three values of α are used, which subsequently provide three different values for β , i.e., $\beta < 1, \beta = 1$ and $\beta > 1$, respectively.

Figs. 7.1 and 7.2 verify the ratio distribution obtained in Theorem 1. The derived result in the theorem has three equations for three different conditions of β . It can be seen that the analytical results for each expression closely match with the simulation results calculated for two different sets of parameters. For each set, three results are calculated and compared for

three different conditions of β . Studying this graph help us understand the effects of parameters on the distribution. Increase in the value of k and θ , saturates the CDF of the ratio at lower values, whereas the effect of β is variable. When k and θ are 1 as in Fig. 7.2, the CDF saturates early with the corresponding increase in the value of β , whereas in the Fig. 7.1, where k and θ are different and greater than 1, the CDF saturates early with the corresponding decrease in the value of β .

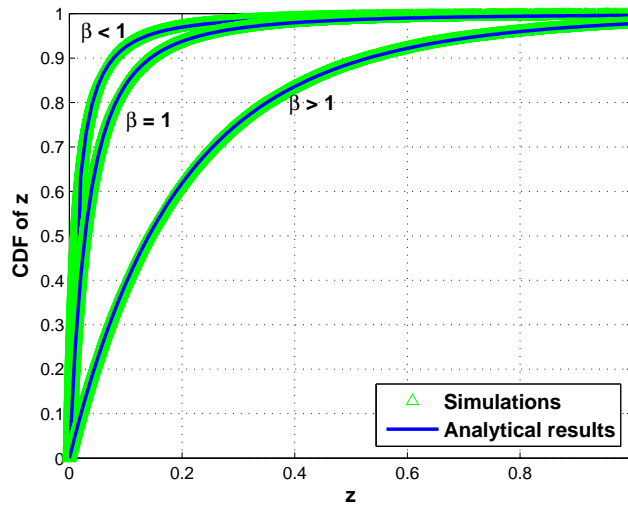


Figure 7.1: CDF of the ratio for $k = 2$, $\theta = 15^\beta$, $\omega = 1$ and $\beta = 0.8, 1, 2$.

Fig. 7.9 shows the trends of the coverage probability of a SISO link versus the SNR margin for various node densities. SNR margin is the normalized threshold defined as $\psi = P_t/\tau$. The effect of the SNR margin and node density on the coverage probability is quite evident. The coverage probability is directly proportional to the SNR margin as well as the node density. Keeping one variable fixed and increasing the other, increases the coverage probability. At low SNR margin, the density of the network plays an important role. For instance, it can be seen that at $5dB$, 16.7% increase in success proba-

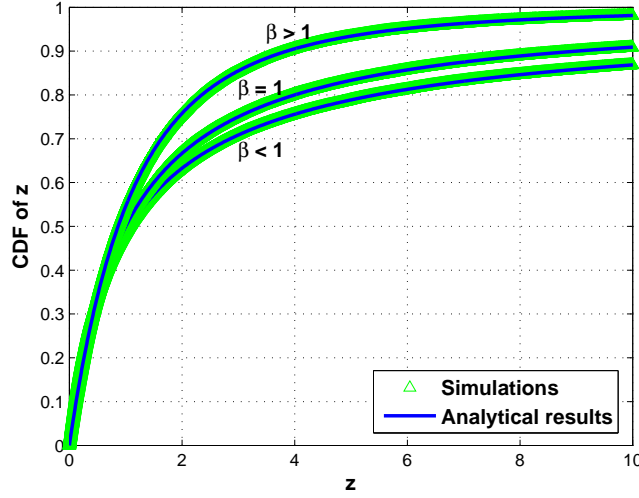


Figure 7.2: CDF of the ratio for $k = 1$, $\theta = 1$, $\omega = 1$ and $\beta = 0.8, 1, 2$.

bility is obtained by doubling the density of the network. Whereas, when λ is increased from 2 to 3, the corresponding increase in success probability is only 5.9%. Hence a trend of diminishing returns can be observed.

For the analysis of the multi-hop SISO network, m -hop success probability is an important parameter, defined as P_s^m , where P_s is the one-hop success probability. The m -hop success probability defines the end-to-end success probability of delivering the message to the m th hop. Normally it is desired that a quality of service (QoS), η , should be maintained in the network where η can be defined as end-to-end success probability for m hops. Hence, $P_s^m \geq \eta$, to guarantee a successful transmission. An upper bound on the number of hops can be evaluated given as

$$m \leq \frac{\ln \eta}{\ln P_s}. \quad (7.1)$$

Fig. 7.4 shows the maximum hop count of a SISO multi-hop network for a specific set of parameters plotted against the SNR margin. Hop count

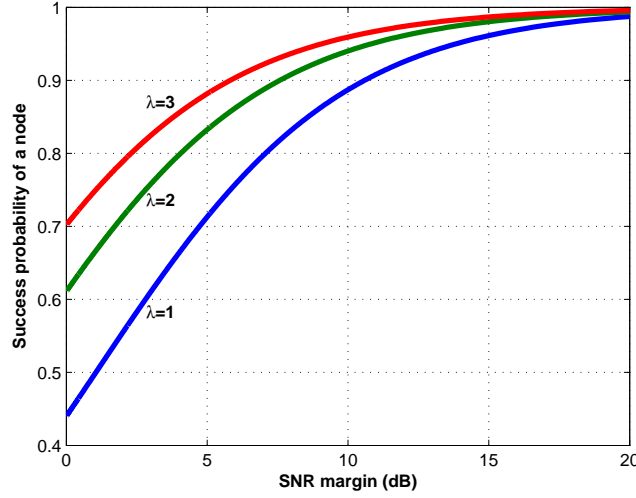


Figure 7.3: Coverage probability of a SISO link for $k = 1$, $\omega = 1$, $\alpha = 2$ and $\beta = 1$.

increases significantly as SNR margin is increased above $25dB$. The maximum hop count also increases with the increasing node density. However, there is a trade off between these two parameters for achieving a specific maximum hop count. For instance, to achieve a hop count of 100, a network with node density of $\lambda = 2$ requires 13.9% less transmit power as compared to $\lambda = 1$ for fixed threshold level. Whereas, the transmit power requirement reduces by 21.8% for a network with a node intensity of $\lambda = 4$ and 17.5% for a node density of $\lambda = 3$, respectively, when compared with a density of $\lambda = 1$. Hence a suitable combination of these parameters can be used for the optimal performance of the multi-hop network.

Fig. 7.5 shows the coverage probability of the SISO network with limited node participation. As discussed previously, when $k = 1$ is used in (4.3), every other node communicates with its first neighboring node. Similarly when $k = 2$, then node communicates with the second neighboring node as shown

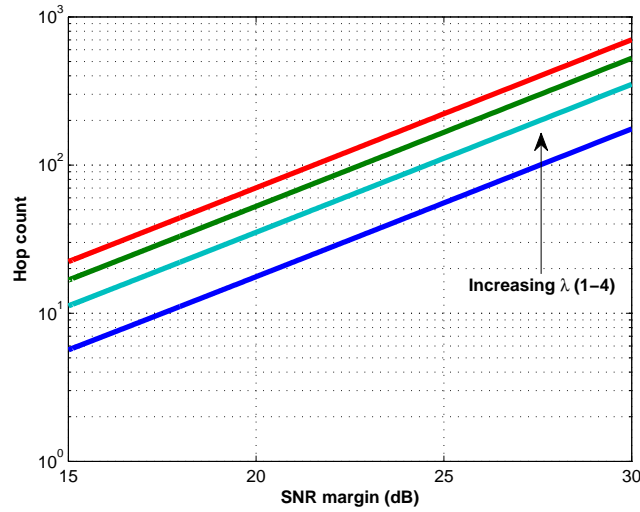


Figure 7.4: Hop count for $k = 1$, $\omega = 1$, $\alpha = 2$, $\beta = 1$ and $\eta = 0.8$.

in Fig. 4.1 and the energy of the first neighboring node can be conserved. This model reduces the energy consumption by a factor of two, provided the coverage probability is above a defined QoS. If node communicates to the third neighboring node, i.e., $k = 3$, then at maximum $2/3$ of the energy of the system will be conserved as long as the coverage probability is above the limit. From Fig. 7.5, at an SNR margin of $11dB$, the coverage probability for both $k = 1$ and $k = 2$ are well above 80% , which is our desired QoS, so alternative nodes can be used for communication and almost 50% of the energy can be conserved. Similarly at an SNR margin of $23dB$, coverage probability for all three cases are almost 100% , so the system will be more energy efficient if $k = 3$ is used as compared to other two values.

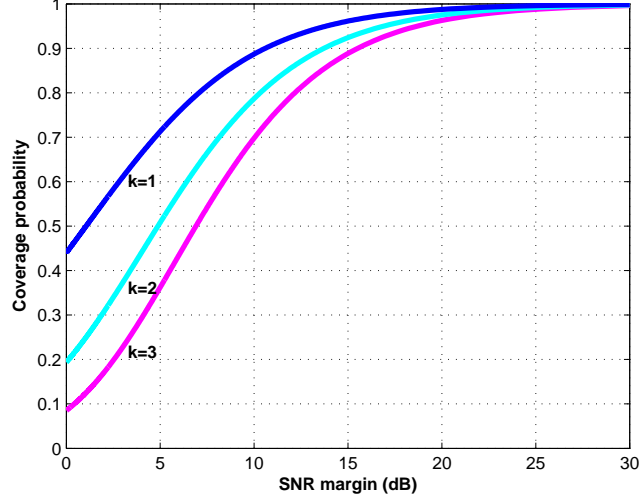


Figure 7.5: Effect of nearest communicating node on the coverage probability for $\lambda = 1$, $\omega = 1$, $\alpha = 2$ and $\beta = 1$.

7.2 MISO Links

In this section, we validate our analytical models that characterize the performance of a virtual MISO network in terms of the coverage probability, one-hop success probability, coverage range and the energy efficiency of the network. We first verify Theorem 2 with hypothetical boundaries. For the sake of simulation results, we take two contiguous squares of length L and distribute nodes using a Poisson RV and calculate the received power at a node in the square using (3.2). We repeat this process for over $1e^5$ iterations and calculate the outage probability by comparing the received power with a certain threshold, τ , when the transmit power of all the nodes is same $P_t = 1$. Fig. 7.6 validates the outage probability expression in (5.3) to that of simulation. To calculate outage probability, received power is compared with a threshold, τ , for 100,000 iterations. Three different nodes intensities

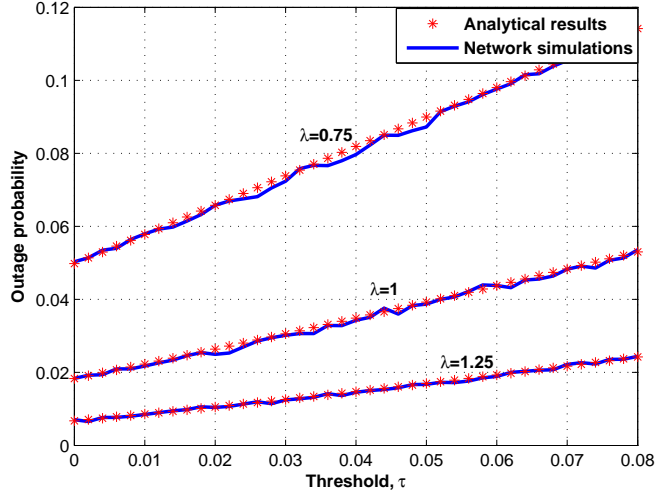


Figure 7.6: Outage probability for virtual MISO with hypothetical boundaries for $P_t = 1$, $L = 2$ and $\alpha = 2$.

0.75, 1 and 1.25 are considered for validation of outage probability expression derived in Theorem 1. All three results match closely with the simulation results. The outage probability increases as τ increases but the increase in outage probability is significant as the node density is decreased from 1 to 0.75. Analytical expression involves infinite summation but accuracy up-to the two decimal points can be achieved from first six terms of the summation.

After verification of the Theorem 2, we move on to the analysis of the virtual MISO network without hypothetical boundaries. Initially we verify our claim of the membership probability function to be Gaussian using Monte-Carlo simulations. For the simulation purpose, we consider a strip-shaped network of length 200 and width 8 in which nodes are distributed uniformly with intensity 0.1125. A source node is placed at the start of the network and it broadcasts the signal. Every other node that receives the signal and

able to successfully decode it, based on threshold, τ , will transmit the signal in the next time slot. The DF nodes that transmit the signal at next time slot form level 1. For the formation of next level, there are multiple copies of the signal receiving at one node and the received power at a receiving node is calculated using (3.2). The nodes with received power greater than τ and which are not part of the previous level (or levels), form next level. This process continues till the signal is broadcasted to the entire network. We observe the decoding pattern of the nodes in the subsequent levels formed at a later stage of the process and calculate the membership probability as shown in Fig. 7.7 by repeating the above process for $1e^5$ iterations. It can be observed that the membership probability follows a Gaussian distribution and the membership probability for the three adjacent levels are almost similar with similar mean and standard deviation. This behavior links to the quasi-stationary phenomenon, which informs that a steady-state is reached when the wave (of transmission) traverses the entire network.

We now compare the distribution of the squared Euclidean distance derived from computer simulations with the Weibull distribution derived in Section ???. For the sake of computer simulations, two nodes are positioned randomly in adjacent levels and x coordinates of node 1 and node 2 are generated according to Gaussian distributions $N(\nu_1, \sigma_1)$ and $N(\nu_2, \sigma_2)$, respectively, where $\mu = \nu_2 - \nu_1$. The parameter μ specifies the hop distance and y coordinates of both nodes are generated according to a uniform distribution, i.e., $U(0, B)$. The squared Euclidean distance is calculated between these two nodes and the process is repeated over $1e^6$ iterations to calculate the resulting PDF. It can be seen from Fig. 7.8 that the analytical results for different values of the hop distance, μ , closely match the simulation results. Hence, the Weibull distribution in (5.29) provides a good approximation for

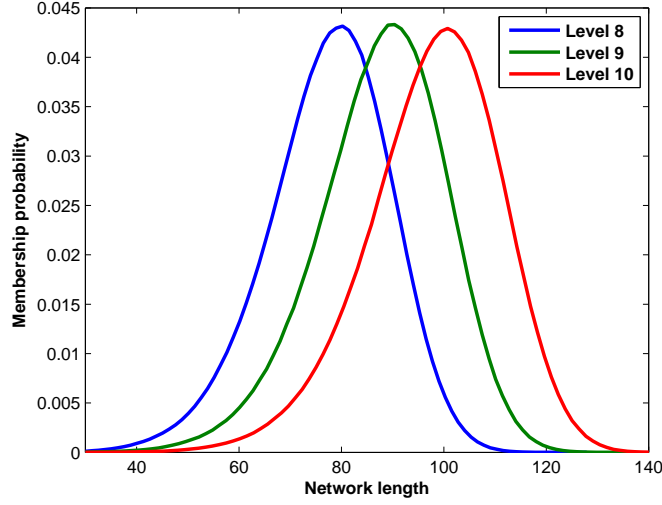


Figure 7.7: Membership probability in three adjacent levels virtual MISO with irregular hop boundaries for $B = 8$, $\tau = 0.04$, $\alpha = 2$.

the squared Euclidean distance. Note that a large value of μ specifies that the two levels are farther apart from each other. Hence the values of the PDF on ordinate become smaller.

Fig. 7.9 validates the analytical expression of the coverage probability in (5.11) for irregular hop boundaries by comparing it to that of simulations. For simulation purpose, a random number of nodes is generated using a Poisson RV in one level and the received power at a node in the next level is calculated with no fixed boundary in between them, using (3.2) and compared with a decoding threshold, τ . The coverage probability at a node is calculated by repeating the process over $1e^5$ iterations. The results are calculated for various values of τ and different average number of nodes γ . It can be noticed that the analytical model provides a close fit to the simulation model. Also we can infer the relationship between coverage probability of a node and the decoding threshold. Coverage decreases as we increase the threshold or

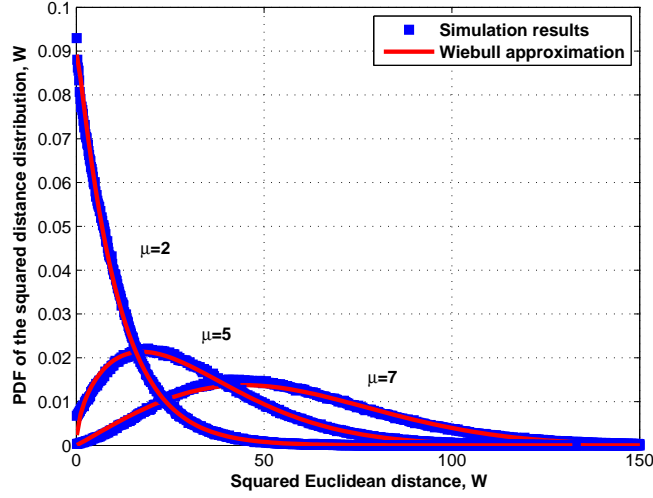


Figure 7.8: Comparison of the simulation distance distribution with the Weibull distribution for virtual MISO with irregular hop boundaries $B = 4$, $\Delta = 2$ and $\alpha = 2$.

decrease the number of nodes per hop. For instance, it can be seen that at $\tau = 0.04$, the coverage probability increases by 5.5% when γ is increased from 3 to 4. Whereas the increase in coverage probability is 2.1% when γ is increased from 4 to 5. Hence a diminishing trend can be observed.

In Fig. 7.10, the one-hop success probability of the random network with different average number of nodes is plotted against the SNR margin, $\psi = P_t/\tau$. It can be observed that the one-hop success probability increases with the increasing node densities for a fixed SNR margin and it also increases as the SNR margin is increased for a fixed node density. It can be seen that the one-hop success probability curves seem to approach a limiting value with the increased SNR margin. This asymptotic limit trace back to the theory of PPP, as the number of nodes at level m can be zero with probability $\exp(-\gamma P_s^m)$, which amounts to a hop failure. These failures can be reduced

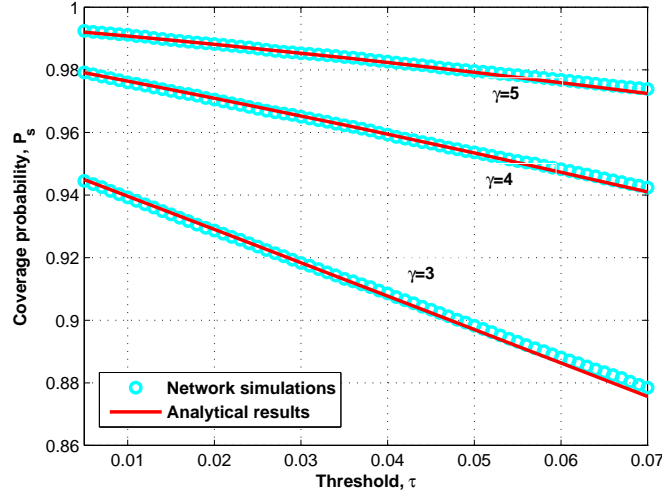


Figure 7.9: Comparison of the coverage probability of a node for MISO without hypothetical boundaries using analytical and simulation model for $B = 4.69$, $\mu = 1.17$, $\Delta = 1.45$, $P_t = 1$ and $\alpha = 2$.

by increasing the node intensities and/or hop area, which in turn reduces the void probability. Hence the node intensities play a vital role in achieving a certain one-hop success probability as compared to SNR margin.

Similarly, in a cooperative multi-hop network, the system performance can be characterized in terms of the m -hop success probability and the coverage range (CR) for which the message propagates while maintaining a QoS, η . If the average number of the DF nodes in the first level after transmission is γP_s , and the average number of the DF nodes at level m is γP_s^m , then the m -hop success probability is calculated as

$$\mathbb{P}(k_n \geq 1) = 1 - \exp(-\gamma P_s^m). \quad (7.2)$$

The QoS, η , which is the desired m -hop success probability, acts as an upper bound on m -hop success probability to calculate the number of the hops

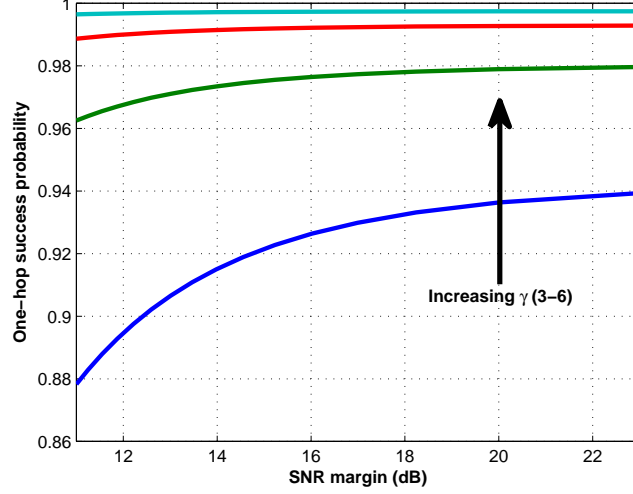


Figure 7.10: Effect of the average number of nodes on one-hop success probability with $\alpha = 2$, $\mu = 2.62$, $\Delta = 2.12$ and $B = 7.87$.

which the signal traverses, i.e., $\mathbb{P}(k_n \geq 1) \geq \eta$. The m -hop success probability in (7.2) is dependent upon the coverage probability, P_s , which is unique for different set of the network parameters (P_t , γ , τ , etc.) and comparing it with η provide the maximum hop count, given as

$$m \leq \frac{\ln[-\ln(1-\eta)/(\lambda|S|)]}{\ln P_s}. \quad (7.3)$$

The average value of CR can then be calculated as

$$CR = m\mu. \quad (7.4)$$

A contour plot of CR against the transmit power, P_t , and the average number of the nodes, γ , is shown in Fig. 7.11, for $\eta = 0.8$ and $\tau = 0.2$. It is observed that the same value of CR can be attained for different set of values of P_t and γ and a network designer can choose any set of parameters depending upon the network constraints and requirements. For instance, it can be seen

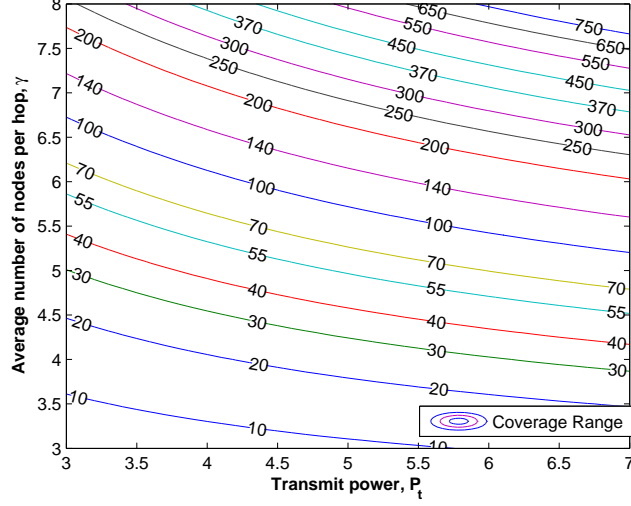


Figure 7.11: Coverage range for different values of transmit power, P_t , and average number of nodes, γ with $\mu = 4.05$, $\Delta = 1.27$, $B = 9.75$, $\eta = 0.8$ and $\tau = 0.2$.

that at $\gamma = 8$, the CR is increased by 278% when P_t is increased from 3 to 7. Whereas, the CR increases by 134% with $\gamma = 4$ for the same increase in transmit power.

We now focus on the results of the energy efficiency for OLA network. Fig. 7.12 shows the FES computed for different values of the CR while maintaining a QoS. For calculating the success probability of the Th-OLA, $\tilde{\mu}$ is used, however, CR is calculated using μ as hop length does not change. It can be seen that the FES decreases with the increasing CR for a particular γ but still a significant amount of energy can be conserved by using the proposed Th-OLA algorithm and network life can be extended. Since the effective diversity gain of the Th-OLA is less as compared to the basic OLA because of limited node participation, the CR of the Th-OLA is also small as compared to the basic OLA, however, to a particular CR, Th-OLA provides

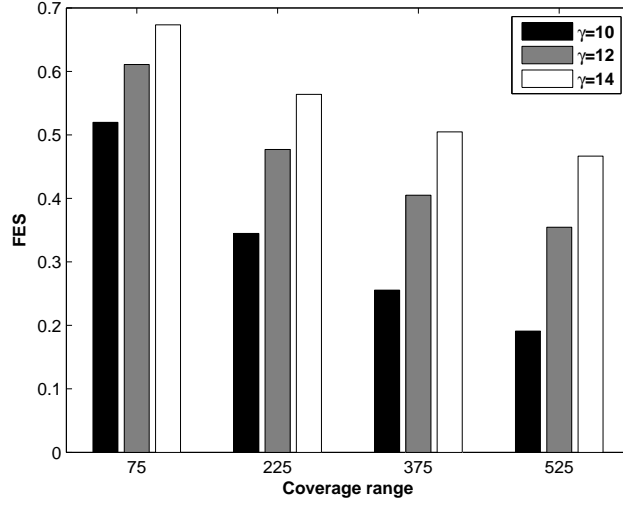


Figure 7.12: FES for three different values of γ with $\mu = 5$, $\psi = 14dB$, $B = 6$, $\eta = 0.8$, and $\Delta = 2$.

an energy efficient approach to achieve that CR. For instance, to achieve a CR of 375, Th-OLA with $\mu = 5$ and $\gamma = 14$ requires 50% less energy as compared to the basic OLA with $\gamma = 14$ and $\mu = 5$ while maintaining the same QoS of 0.8. Hence Th-OLA is successful in saving the energy and extending the life time of the energy constraint networks.

Hop distance is an important factor in characterizing the energy requirements to achieve a particular CR. OLAs with different hop distances require different number of the hops to achieve the same CR. Similarly, Th-OLAs with different hop distances require different number of the hops to achieve the same CR, so the FES for the comparison of two Th-OLAs with different hop distances, i.e., μ_1 and μ_2 , is calculated with the modified version of (6.8), given as

$$FES = 1 - \frac{P_t m \gamma_{t1}}{P_t n \gamma_{t2}} = 1 - \frac{m \gamma_{t1}}{n \gamma_{t2}}, \quad (7.5)$$

where m and n are the number of hops required to achieve a particular CR with two different Th-OLAs of (γ_{t1}, μ_1) and (γ_{t2}, μ_2) , respectively. The Th-OLA with larger hop distance, $\mu = 8$, is compared to the Th-OLA with smaller hop distance, $\mu = 5$ and results are summarized in Table 7.1. These results are calculated for SNR margin, $\psi = 14dB$, with network width, $B = 6$, $\eta = 0.8$ and $\Delta = 2$. OLA with smaller hop distance can achieve a higher CR as compared to larger hop distance as increase in the hop distance increases the path loss attenuation. However, the network with larger hop distance, μ , provides more energy efficient approach in achieving a particular CR for a fixed γ and thus saves a considerable amount of the energy at higher SNR margins. A large hop distance implies that the CR can be achieved in lesser number of the hops. Hence, the total energy requirements for larger hop distances at higher SNR margins are less as compared to smaller hop distances, where more number of hops are required to achieve the same CR. For instance, to achieve a CR of 200, Th-OLA with $\mu = 8$ requires 20% less total energy as compared to Th-OLA with $\mu = 5$ for $\gamma = 14$ and $\psi = 14dB$. Hence, larger hop distances are more energy efficient at higher SNR margins and also reduces the latency of the networks.

The performance of our proposed thinning algorithm is also compared with the independent thinning algorithm of a PPP and the results are shown in Fig. 7.13. In independent thinning, random nodes are deleted independently in one level with probability $1 - p$ and the remaining nodes are allowed to transmit with probability p . The process after thinning still follows another PPP with reduced intensity $p\lambda$ and same area, whereas in our proposed algorithm the effective area of the hop reduces keeping the intensity intact. It can be observed that at lower values of CR, our proposed algorithm and the independent thinning process are almost similar but as the values of

Table 7.1: Effect of hop distance on FES

γ	CR	Energy of Th-OLA (dB)		FES
		$\mu = 5$	$\mu = 8$	
10	120	21.2	20.3	0.1898
	200	24	23.2	0.1817
14	120	21	19.9	0.2085
	200	23.8	22.8	0.2043

CR increases, our algorithm outperforms independent thinning. The success probability for independent thinning approach is calculated using μ , as the hop area does not change, whereas for Th-OLA, $\tilde{\mu}$ is used, which effectively reduces the effect of the path loss for the Th-OLA. For instance, to achieve a CR of 100, Th-OLA requires 11.8% less energy than independent thinning. Hence Th-OLA is more energy efficient than independent thinning algorithm for the considered strip-shaped network.

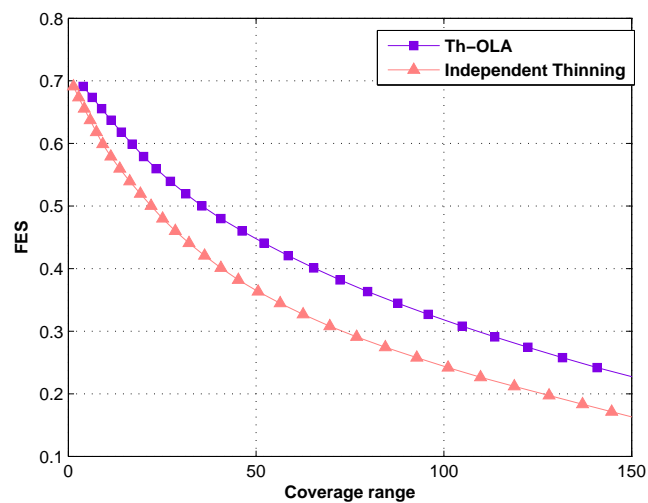


Figure 7.13: Comparison of the Th-OLA with the independent thinning process for $\psi = 14dB$, $\gamma = 8$, $\mu = 5$, $\Delta = 2$, $\eta = 0.8$ and $B = 6$.

Chapter 8

Conclusion and Future

Direction

We have developed and analyzed a spatial Poisson point process model for a strip-shaped multi-hop network with random number of nodes and irregular hop boundaries in the presence of path loss and Rayleigh fading for SISO links and for virtual MISO links. In SISO links, GG distribution is used to model the distance and the ratio distribution of the exponential RV and GG RV has been derived, which is used to determine the coverage probability of a node. The Euclidean distance distribution between two randomly located nodes in adjacent levels is derived for MISO links and approximated with the Weibull distribution for a tractable solution. A closed-form expression for the PDF of the received power at a node for MISO links is derived by self convolution of the ratio of an exponential RV and a Weibull RV over a PPP. The received power distribution is used to analyze the network in terms of the coverage range and one-hop success probability. We proposed an energy efficient algorithm for MISO networks based upon the thinning of the total transmitters in one level. It is shown that our algorithm saves a significant

amount of energy when compared with basic OLA and it is more efficient than independent thinning.

A future direction of this work would be to study the OLA network under following conditions

- Shadowing-Effect of shadowing is modeled with an other RV which will change the received power distribution. Derivation of the received power distribution would be an important study.
- Variable transmit power-Since we use same transmit power for all relaying nodes, a significant contribution to this work would be addition of the effects of the variable transmit power

Bibliography

- [1] A. Sendonaris, E. Erkip, and B. Aazhang, “User cooperation diversity. part i. system description,” *IEEE Trans. Wireless Commun.*, vol. 51, no. 11, pp. 1927-1938, 2003.
- [2] J. N. Laneman, D. N. Tse, and G. W. Wornell, “Cooperative diversity in wireless networks: Efficient protocols and outage behavior,” *IEEE Trans. Inf. Theory*, vol. 50, no. 12, pp. 3062-3080, 2004.
- [3] S. Lakshmanan and R. Sivakumar, “Diversity routing for multi-hop wireless networks with cooperative transmissions,” *IEEE SECON*, pp. 1-9, 2009.
- [4] X. Tao, X. Xu, and Q. Cui, “An overview of cooperative communications,” *IEEE Commun. Magazine*, vol. 50, no. 6, pp. 6571, 2012.
- [5] A. Scaglione and Y. W. Hong, “Opportunistic large arrays: cooperative transmission in wireless multihop ad hoc networks to reach far distances,” *IEEE Trans. Signal Process.*, vol. 51, no. 8, pp. 2082-92, Aug. 2003.
- [6] M. Haenggi, and R. K. Ganti, *Interference in Large Wireless Networks*, Now Publishers Inc., 2009.

- [7] S. A. Hassan and M. A. Ingram, "A quasi-stationary markov chain model of a cooperative multi-hop linear network," *IEEE Trans. Wireless Commun.*, vol. 10, no. 7 pp. 2306-2315, July 2011.
- [8] L. Sankaranarayanan, G. Kramer, and N. B. Mandayam, "Cooperative diversity in wireless networks: A geometry-inclusive analysis," *Annual ACCCC*, pp. 1598-1607, Sept. 2005.
- [9] S. A. Hassan and P. S. Wang, "A dual relay transmission system for wireless communications: Power allocations and channel capacity," *IEEE Intl. Wireless and Microwave Technology Conference (WAMICON)*, pp. 1-4, Apr. 2009.
- [10] K. Victor, Y. Wu, and Y. Li, "Error rate performance in OFDM-based cooperative networks," *IEEE Global Communication Conference (GLOBECOM)*, pp. 3447-3451. Nov. 2007.
- [11] M. Bacha and S. A. Hassan, "Distributed versus cluster-based cooperative linear networks: A range extension study in suzuki fading environments," *IEEE Personal Indoor and Mobile Radio Commun. (PIMRC)*, Sept. 2013.
- [12] S. A. Hassan, "Range extension using optimal node deployment in linear multi-hop cooperative networks," *IEEE Radio and Wireless Symposium (RWS)*, pp. 364-366, Jan. 2013.
- [13] A. Bletsas, A. Khisti, D. P. Reed, and A. Lippman, "A simple cooperative diversity method based on network path selection," *IEEE J. Sel. Areas Commun.*, vol. 24, pp. 659-672, Mar. 2006.

- [14] A. Bletsas, H. Shin, and M. Z. Win, "Cooperative communications with outage-optimal opportunistic relaying," *IEEE Trans. Wireless Commun.*, vol. 6, pp. 3450-3460, Sept. 2007.
- [15] W. Ye, J. Heidemann, and D. Estrin, "An energy-efficient mac protocol for wireless sensor networks," *IEEE INFOCOM*, vol. 3, pp. 1567-1576, 2002.
- [16] Y.-W. Hong and A. Scaglione, "Energy-efficient broadcasting with cooperative transmissions in wireless sensor networks," *IEEE Trans. Wireless Commun.*, vol. 5, no. 10, pp. 2844-2855, 2006.
- [17] M. Hussain and S. A. Hassan, "Performance of multi-hop cooperative networks subject to timing synchronization errors," *IEEE Trans. Commun.*, vol. 63, no. 3, pp. 655-666, March 2015.
- [18] B. Sirkeci-Mersen and A. Scaglione, "A continuum approach to dense wireless networks with cooperation," *IEEE INFOCOM*, vol. 4, pp. 2755-2763, Mar. 2005.
- [19] H. Jung and M. Weitnauer, "Multi-packet interference in opportunistic large array broadcasts over disk networks," *IEEE Trans. Wireless Commun.*, vol. 12, no. 11, pp. 5631-5645, 2013.
- [20] C. Capar, D. Goeckel, and D. F. Towsley, "Broadcast analysis for large cooperative wireless networks," *CoRR*, vol. abs/1104.3209, 2011.
- [21] S. A. Hassan and M. A. Ingram, "A quasi-stationary markov chain model of a cooperative multi-hop linear network," *IEEE Trans. Wireless Commun.*, vol. 10, no. 7 pp. 2306-2315, July 2011.

- [22] M. Bacha and S. A. Hassan, "Performance analysis of cooperative linear networks subject to composite shadowing fading," *IEEE Trans. Wireless Commun.*, vol. 12, no. 11, pp. 5850-5858, 2013.
- [23] Q. Shafi and S. A. Hassan, "Interference analysis in cooperative multi-hop networks subject to multiple flows," *Proceedings of the IEEE/IFIP Wireless Days*, Nov. 2014.
- [24] S. S. Syed and S. A. Hassan, "On the use of space-time block codes for opportunistic large array network," *IEEE International Wireless Communications and Mobile Computing Conference (IWCMC)*, Aug. 2014.
- [25] M. Bacha and S. A. Hassan, "Coverage aspects of cooperative multi-hop line networks in composite fading environment," *IEEE International Wireless Communications and Mobile Computing Conference (IWCMC)*, Aug. 2014.
- [26] M. Bacha and S. A. Hassan, "Coverage aspects of cooperative multi-hop line networks in correlated shadowed environment," *IEEE International Conference on Computing, Networking and Communications (ICNC)*, Feb. 2014.
- [27] S. A. Hassan and M. A. Ingram, "Analysis of an opportunistic large array line network with bernoulli node deployment," *IET Communications*, vol. 8, no. 1, pp. 19-26, 2014.
- [28] A. Afzal and S. A. Hassan, "Stochastic modeling of cooperative multi-hop strip networks with fixed hop boundaries," *IEEE Trans. Wireless Commun.*, vol. 13, no. 8, pp. 4146-4155, Aug. 2014.
- [29] S. A. Hassan, "Performance analysis of cooperative multi-hop strip networks," *Wireless Personal Commun.*, vol. 74, no. 2, pp. 391- 400, 2014.

- [30] M. Bacha and S. A. Hassan, "Performance analysis of cooperative linear networks subject to composite shadowing fading," *IEEE Trans. Wireless Commun.*, vol. 12, no. 11, pp. 5850-5858, Nov. 2013.
- [31] D. Moltchanov, "Survey paper: Distance distributions in random networks," *Ad Hoc Net.*, vol. 10, pp. 11461166, Aug. 2012.
- [32] M. Haenggi, "On distances in uniformly random networks," *IEEE Trans. Inf. Theory*, vol. 51, no. 10, pp. 3584-3586, Oct. 2005.
- [33] A. Afzal and S. A. Hassan, "A stochastic geometry approach for outage analysis of ad hoc SISO networks in Rayleigh fading," *IEEE Global Communication Conference (GLOBECOM)*, Dec. 2013.
- [34] L. V. Thanayankizil and A. Kailas, "Energy-efficient strategies for cooperative communications in wireless sensor networks," *IEEE SENSOR-COMM*, pp. 541-546, 2007.
- [35] A. Kailas and M. A. Ingram, "Ola with transmission threshold for strip networks," *IEEE Military Communications Conference (MILCOM)*, pp. 1-7, 2009.
- [36] A. Kailas, "Establishing performance bounds for alternating cooperative broadcasts under high path-loss," *IEEE GLOBECOM Workshops (GC Wkshps)*, pp. 1153-1157, 2011.
- [37] S. A. Hassan and M. A. Ingram, "Snr estimation for a non-coherent m-fsk receiver in a slow flat fading environment," *IEEE International Conference on Communications (ICC)*, pp. 1-5, 2010.

- [38] B. Sirkeci-Mersen and A. Scaglione, "A continuum approach to dense wireless networks with cooperation," *IEEE INFOCOM*, vol. 4, pp. 2755-2763, 2005.
- [39] A. Kailas and M. A. Ingram, "Equitable energy consumption during repeated transmissions in a multihop wireless network," *IEEE Global Telecommunications Conference (GLOBECOM)*, pp. 1-5, 2010.
- [40] L. V. Thanayankizil, A. Kailas, and M. A. Ingram, "Opportunistic large array concentric routing algorithm (OLACRA) for upstream routing in wireless sensor networks," *Ad Hoc Net.*, vol. 9, no. 7, pp. 1140-1153, 2011.
- [41] R. I. Ansari and S. A. Hassan, "Opportunistic large array with limited participation: An energy-efficient cooperative multi-hop network," *IEEE International Conference on Computing, Networking and Communications (ICNC)*, pp. 831-835, 2014.
- [42] E.S. Sousa and J.A. Silvester, "Optimum transmission ranges in a direct sequence spread-spectrum multi-hop packet radio network," *IEEE J. Sel. Areas Commun.*, vol. 8, no. 5, pp. 762-771, Jun 1990.
- [43] A. Kostin, "Probability distribution of distance between pairs of nearest stations in wireless network," *IET Electronics Lett.*, vol. 46, no. 18, pp. 1299-1300, 2010.
- [44] M. K. Simon, *Probability Distributions involving Gaussian Random Variables: A handbook for Engineers and Scientists*. Springer Science and Business Media, 2007.